

# **GNSS Reflectometry Fundamentals**

Prof. James L Garrison  
Purdue University

*African Capacity Building Workshop  
on Space Weather Effects on GNSS  
ICTP, Trieste, Italy  
11 October, 2022*



**Bistatic** radar with **passive** receiver.

Re-use of transmissions from **non-cooperative sources** operated for other purposes (e.g. **navigation** or **communications**)

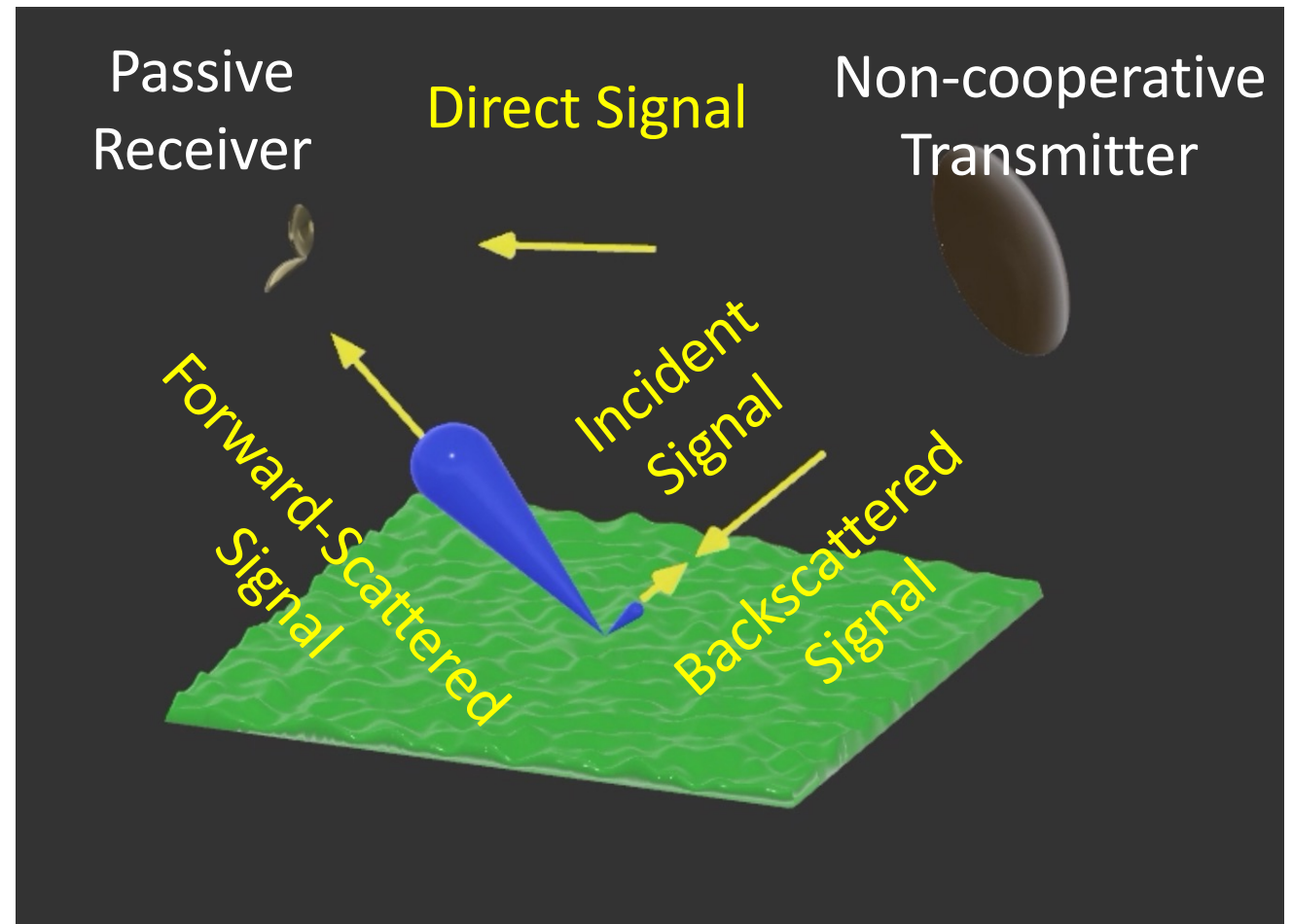
## Definitions:

- GNSS-R = Global Navigation Satellite System Reflectometry
- SoOp-R = Signals of Opportunity Reflectometry

$$\text{GNSS+R} = \{\{\text{GNSS-R}\} \cup \{\text{SoOp-R}\}\}$$



- **Observables:**
  - **Reflectivity**
  - **Phase**
  - **Coherence**
  - **Delay-Doppler Map (DDM)**
- **Geophysical Retrievals:**
  - **Ocean winds**
  - **Altimetry (SSH)**
  - **Surface Soil Moisture**
  - **Wetlands extent**
  - **Sea Ice extent**
  - **Biomass (AGB), etc ...**





## A brief history



# Pre-history of Reflectometry

[Tyler & Simpson (1970) Radio Science [10.1029/RS005i002p00263](#)  
Tyler (1968) JGR [10.1029/JB073i024p07609](#)]

- Scatter of comm. link from Moon (Explorer-35) received at Earth.
- Estimate of Regolith thickness and large-scale surface roughness

[Sutton, et al.,(1973) [10.1109/TCOM.1973.1091693](#)]

- Satellite to Aircraft – study of ocean scatter multipath effects on communications
- Show relationship between bandwidth & roughness

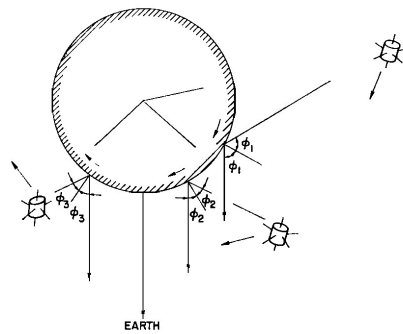


Fig. 1. Experimental geometry of moon and spacecraft.

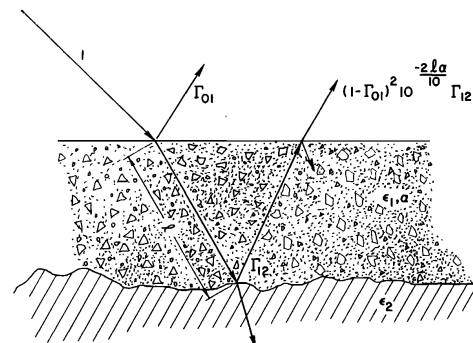


Fig. 8. Model for incoherently reflecting layers.

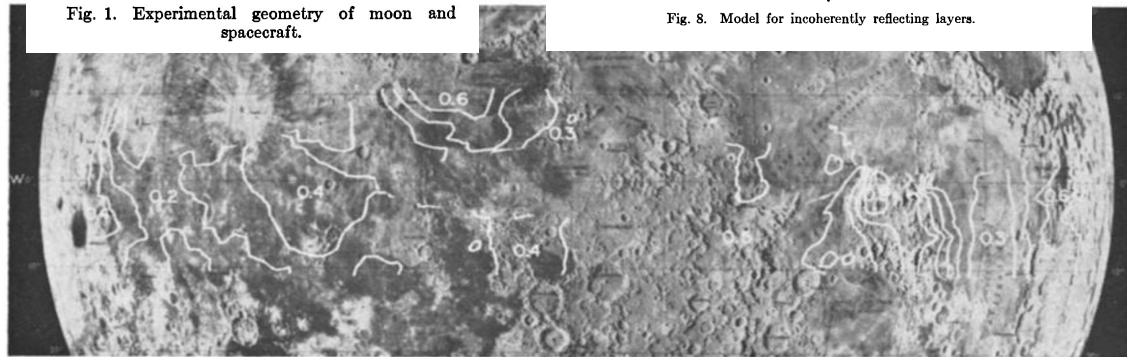
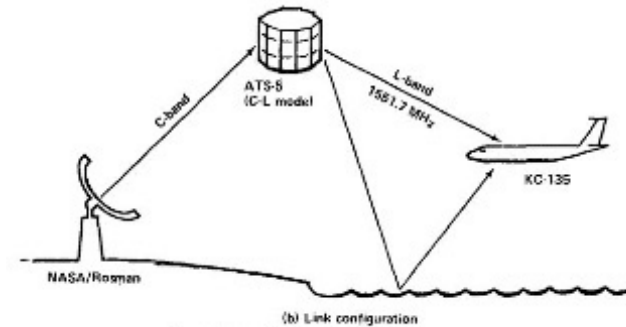


Fig. 4. Slope contours normalized to 0.1 radian. The 0.3 in Mare Fecunditatis indicates values of  $h_0/d_0$  between 0.03 and 0.04 ( $1.7^\circ$  to  $2.2^\circ$ ) unidirectional rms slope. Only those contours within 0.1 lunar radius of data points (cf. Figure 1) are shown.



(b) Link configuration

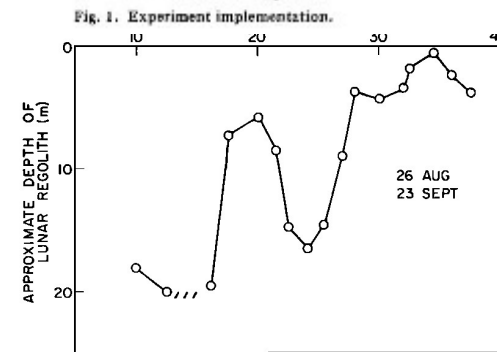
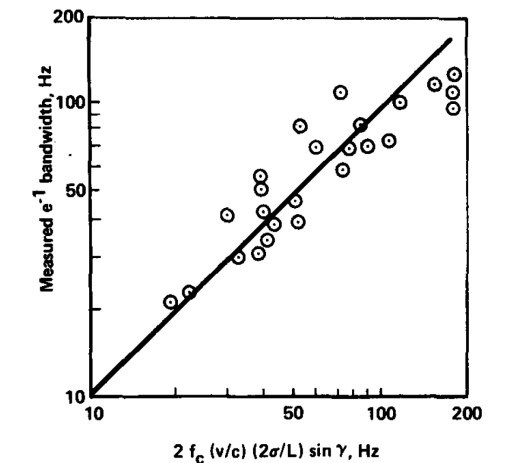
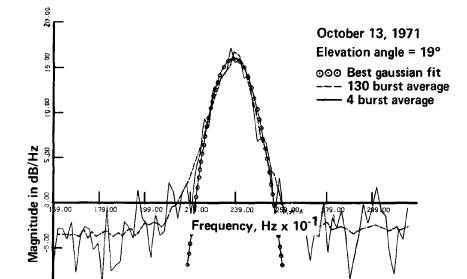


Fig. 9. Estimated depth of lunar debris for tracks of August 26 and September 23, 1967.



# Pre-history of Reflectometry(2)

[Hall & Cordey, (1988)  
10.1109/IGARSS.1988.570200]

- Ocean scatterometry using GPS **backscatter**
- “incapable of giving useful performance”

[Auber, et al., (1994) ION GPS]

- Observed ocean-reflected signals tracked by airborne receiver – leading to navigation solution errors
- First look at modeling rough surface scattering effect on PRN-coded signals

BACKSCATTER CROSSSECTION			Ep (%)		
$\sigma_p^0$ (dB)			GPS	POSSIBLE	NEW SYSTEM
			C/A code	C/A code	long code
0			23	13	2
-5			45	13	2
-10			113	14	3
-15			563	16	6
-20			1011	23	13

SYSTEM PARAMETERS					
name	symbol	unit			
Transmit Power	$P_{Tx}$	(W)	25	2500	2500
Code Length	$M_{code}$	(-)	1023	1023	long
No of Transmitters	$n_{Tx}$	(-)			3
Losses (Tx)	$L_{Tx}$	(dB)			1.5
Pulse Length	$\tau_p$	( $\mu$ s)			1
Ground Resolution	$\rho_g$	(m)			300
Incidence Angle	$i$	(deg)			50
Wavelength	$\lambda$	(m)			0.19
Range, Rx to ground	$R$	(km)			1150
Integration time	$\tau_i$	(ms)			22
Losses (at)	$L_{at}$	(dB)			0.5
Eff Signal Window	$\tau_{obs}$	( $\mu$ s)			595
Eff Noise Window	$\tau_{noise}$	( $\mu$ s)			595
Antenna Diameter	$D$	(m)			4
Losses (Rx)	$L_{Rx}$	(dB)			1.0
Noise Figure	$F_N$	(dB)			2.0

TABLE 1 PERFORMANCE OF CANDIDATE SCATTERMETERS

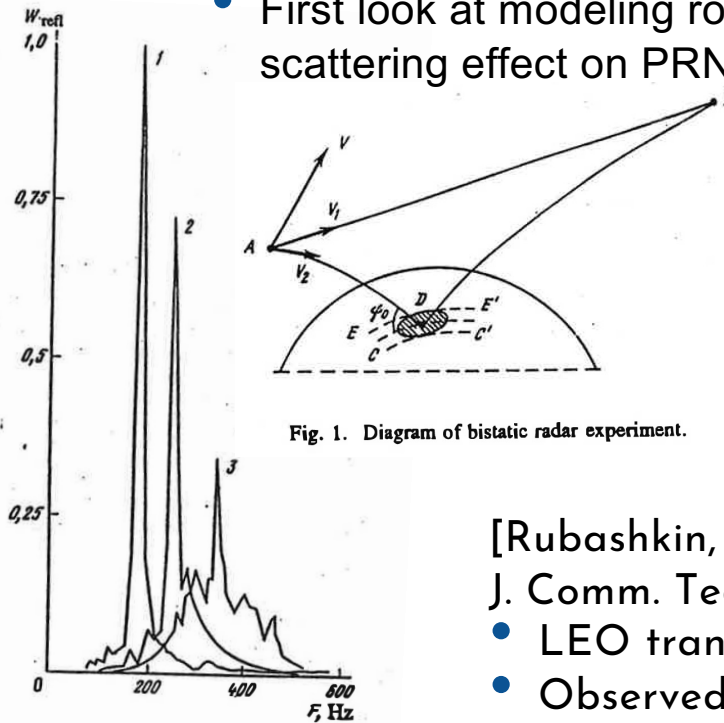


Fig. 2. Typical reflected signal spectra.

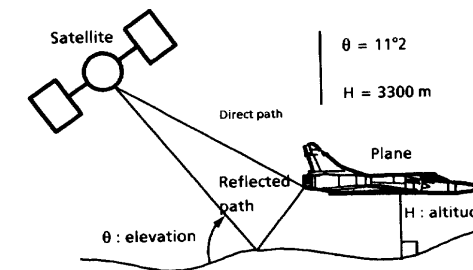
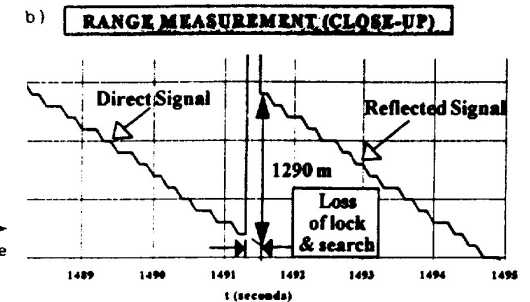
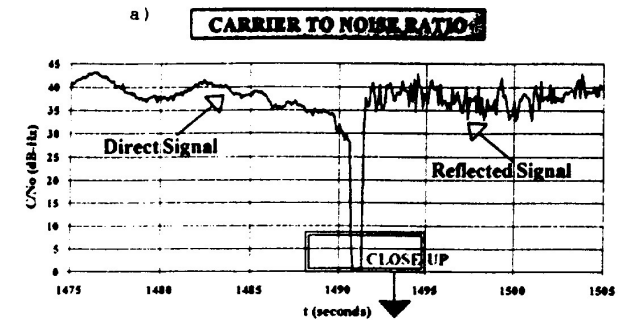
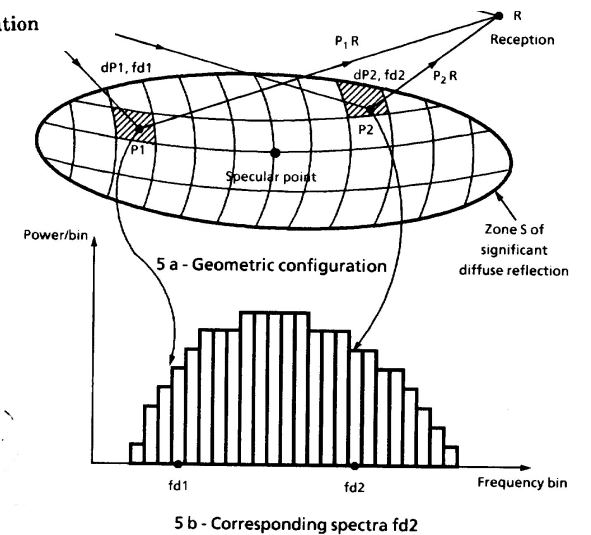


Figure 2: Geometrical configuration

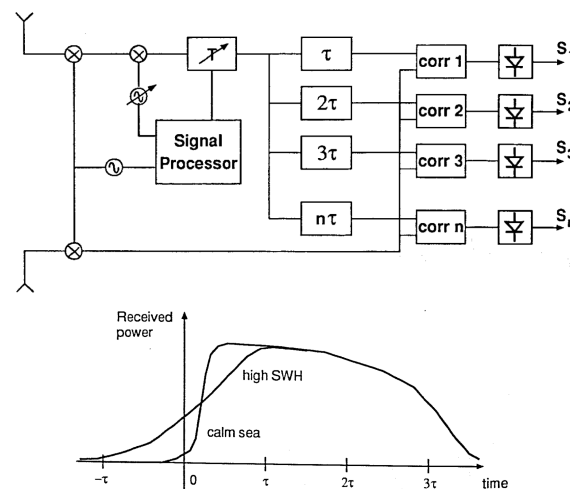
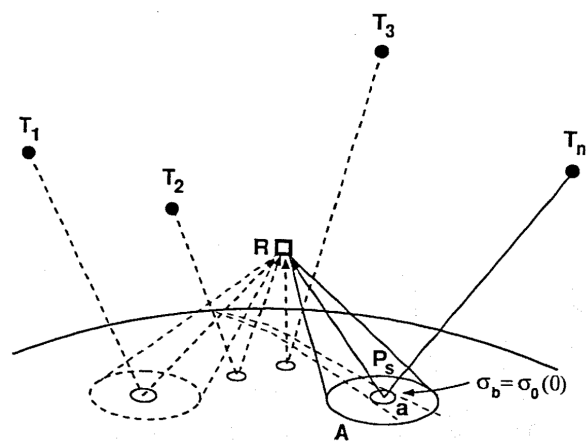
[Rubashkin, et al.,  
J. Comm. Tech. & Elec. 1993]

- LEO transmitter, GEO receiver.
- Observed spectrum widening on ocean reflection



*...as presently used*

- Forward scatter
- Delay-Doppler correlation



[Martin-Neira, M. (1993) ESA Journal]

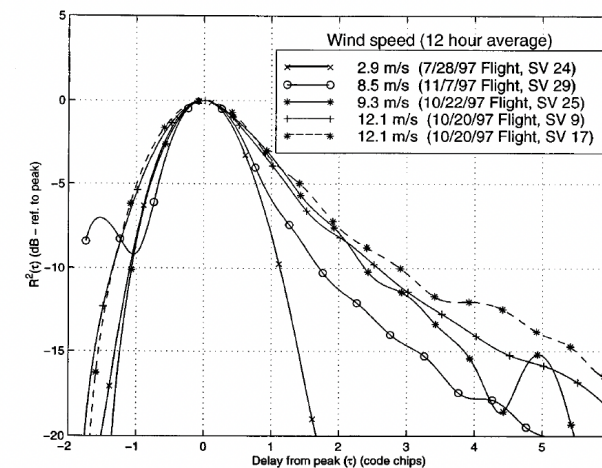
- GNSS Altimetry
- Identified many of the key features developed later



NASA Technical Memorandum 4750

## Utilizing GPS To Determine Ionospheric Delay Over the Ocean

Stephen J. Katzberg and James L. Garrison, Jr.  
Langley Research Center • Hampton, Virginia



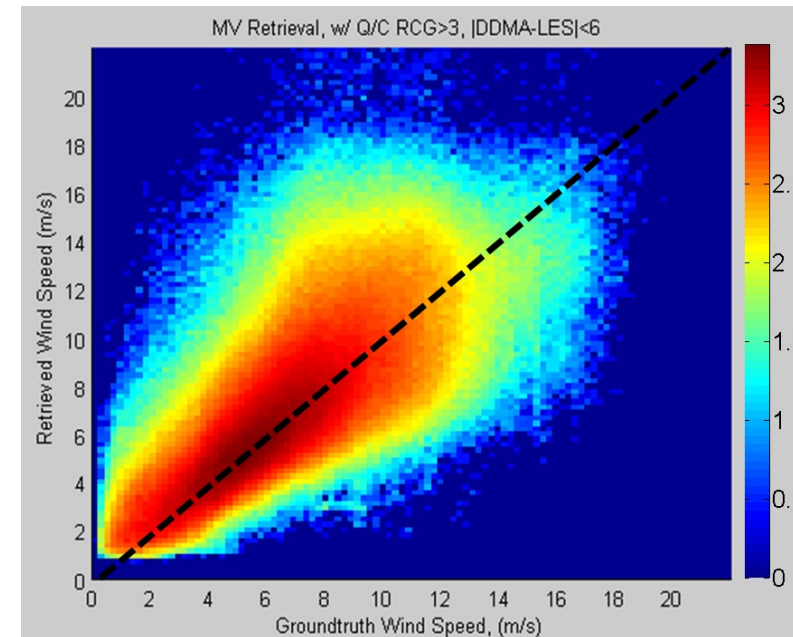
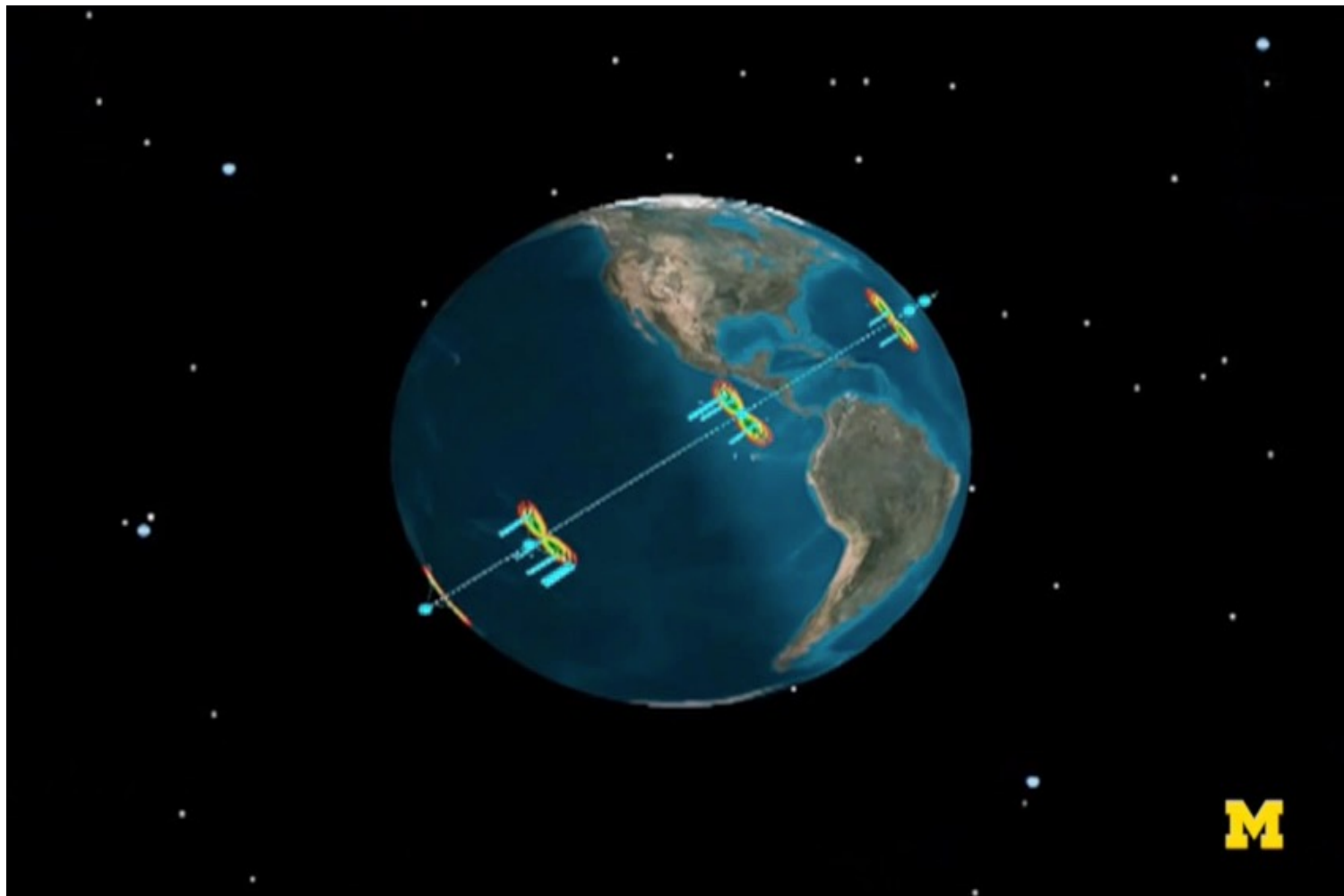
[Katzberg & Garrison NASA TM-4750 (1996)]

[Garrison, et al., GRL (1998), 10.1029/98GL51615]

- Prototype receiver
- First measurements of DDM “spreading” with roughness



# CYGNSS (Launch 2016)



[JSTARS, 2018,  
DOI:10.1109/JSTARS.2018.2833075]



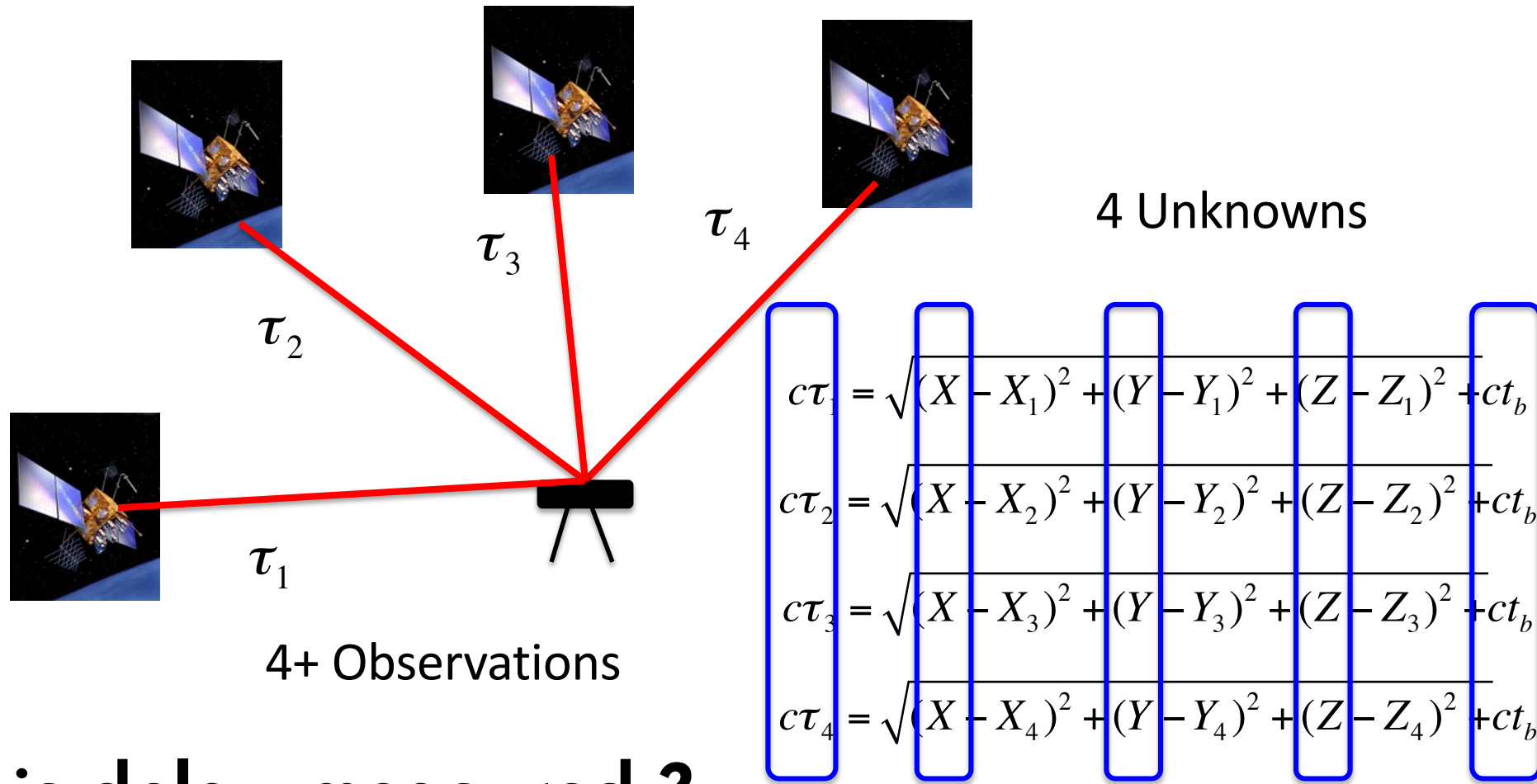
[https://www.youtube.com/watch?time\\_continue=1&v=rRBqn6JPtv8](https://www.youtube.com/watch?time_continue=1&v=rRBqn6JPtv8)



# Fundamentals of GNSS (review)



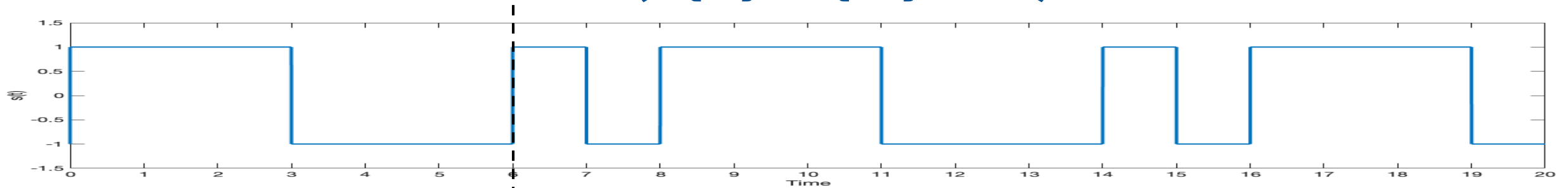
# Fundamentals of GNSS



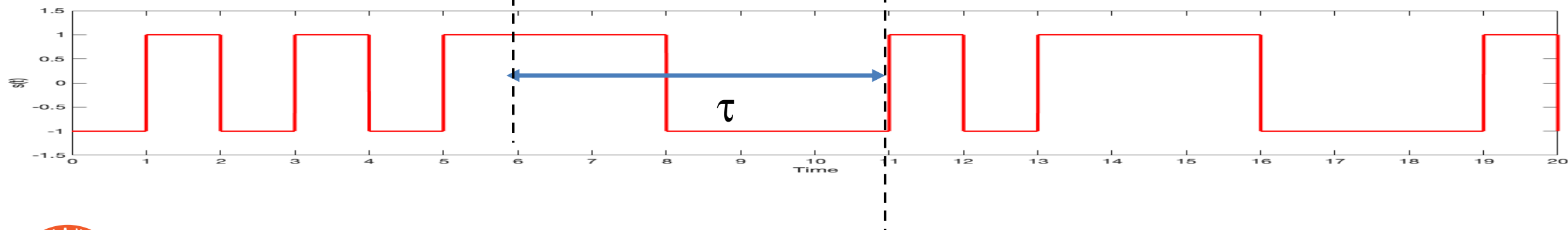
How is delay measured ?

# How is delay measured ?

Transmitter: Ideal *infinitely-long, random* sequence of pulses  
( $P\{-1\}=P\{+1\}=0.5$ )



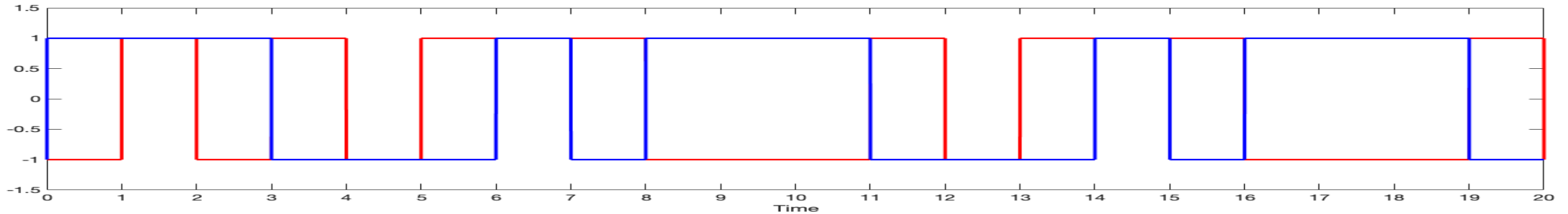
Delay ( $\tau$ ) in propagation to receiver:



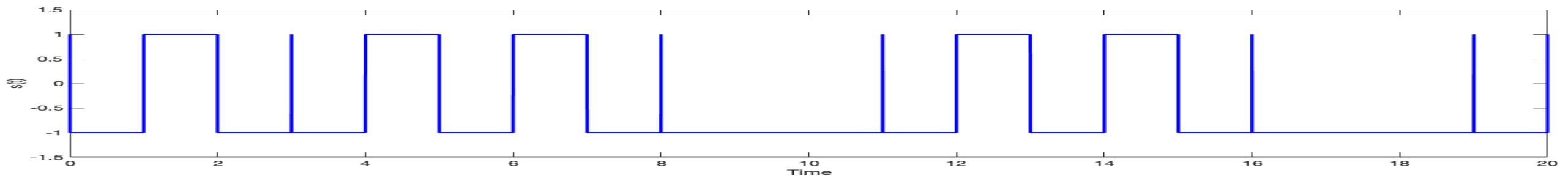


# How is delay measured ?

Receiver - generates *identical local copy* of signal (blue)



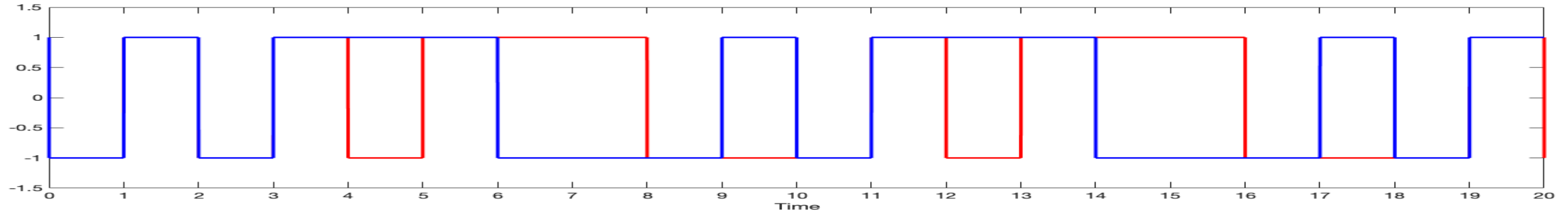
Multiplies it with received signal (red)



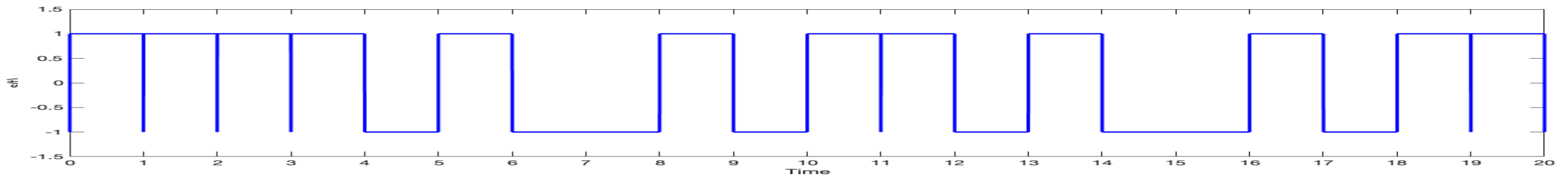
For product:  $P\{-1\}=P\{+1\}=0.5$ , **Sum=0**

# How is delay measured ?

Receiver - varies delay of local copy (blue)



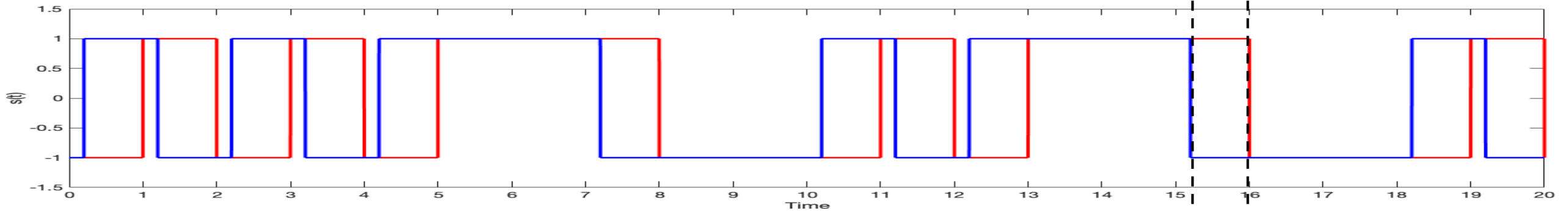
Multiplies it with received signal (red)



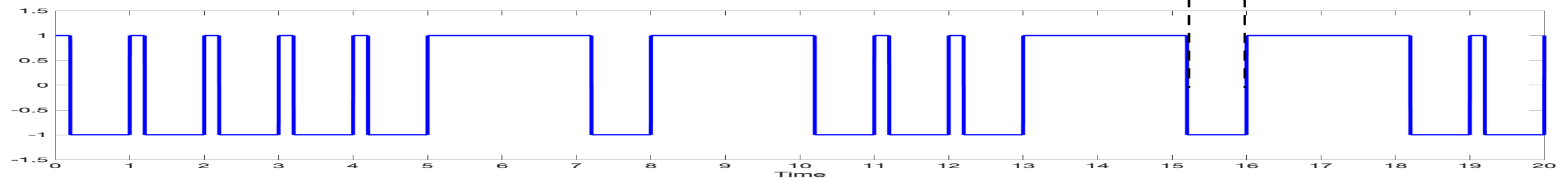
$$\tau = 1 T_c: P\{-1\} = P\{+1\} = 0.5, \text{ Sum} = 0$$

# How is delay measured ?

Receiver - varies delay of local copy (blue)



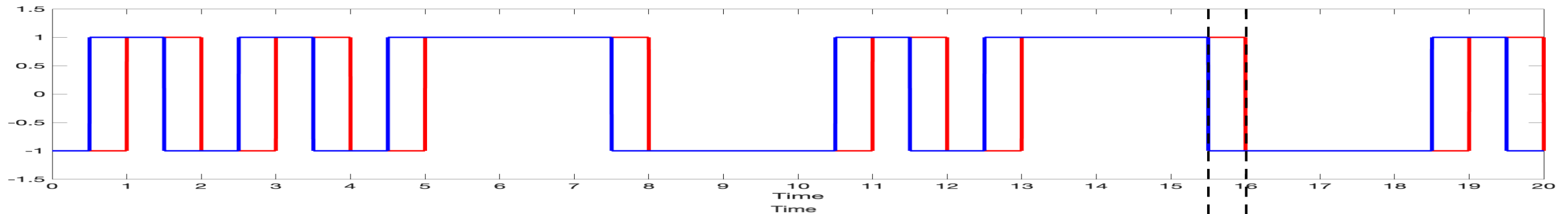
Multiplies it with received signal (red)



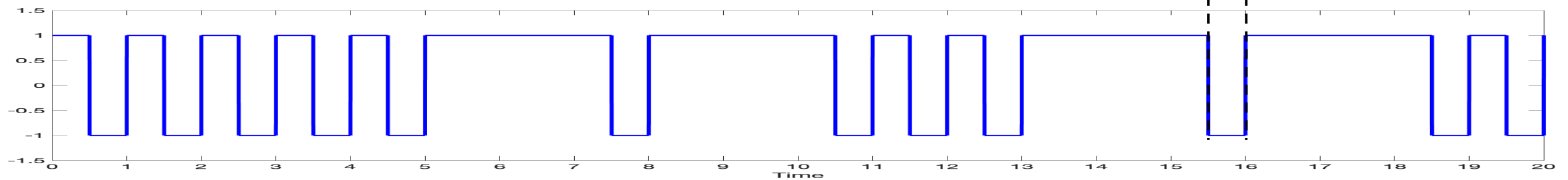
$$\tau = 0.9 T_c: \text{Sum} = 0.1(1) + 0.9(0) = 0.1$$

# How is delay measured ?

Receiver - varies delay of local copy (blue)



Multiplies it with received signal (red)

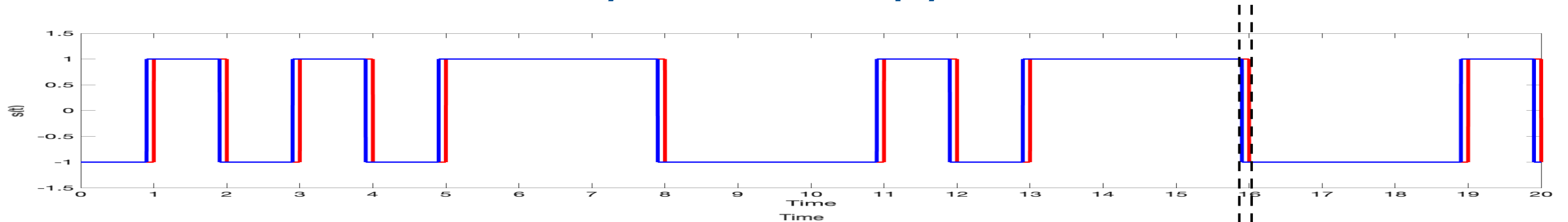


$$\tau = 0.5 T_c: \text{Sum} = 0.5(1) + 0.5(0) = \mathbf{0.5}$$

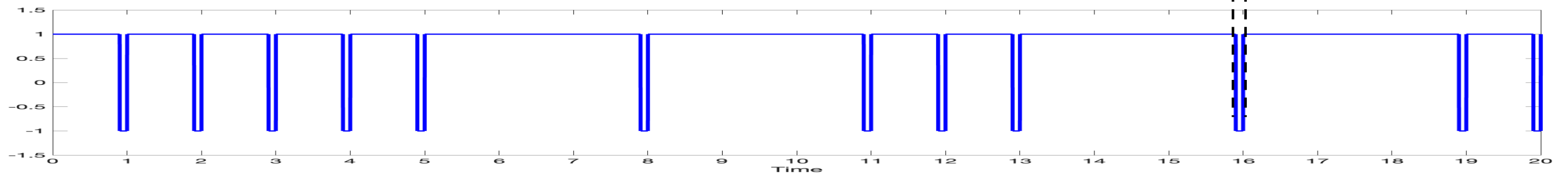


# How is delay measured ?

Receiver - varies delay of local copy (blue)



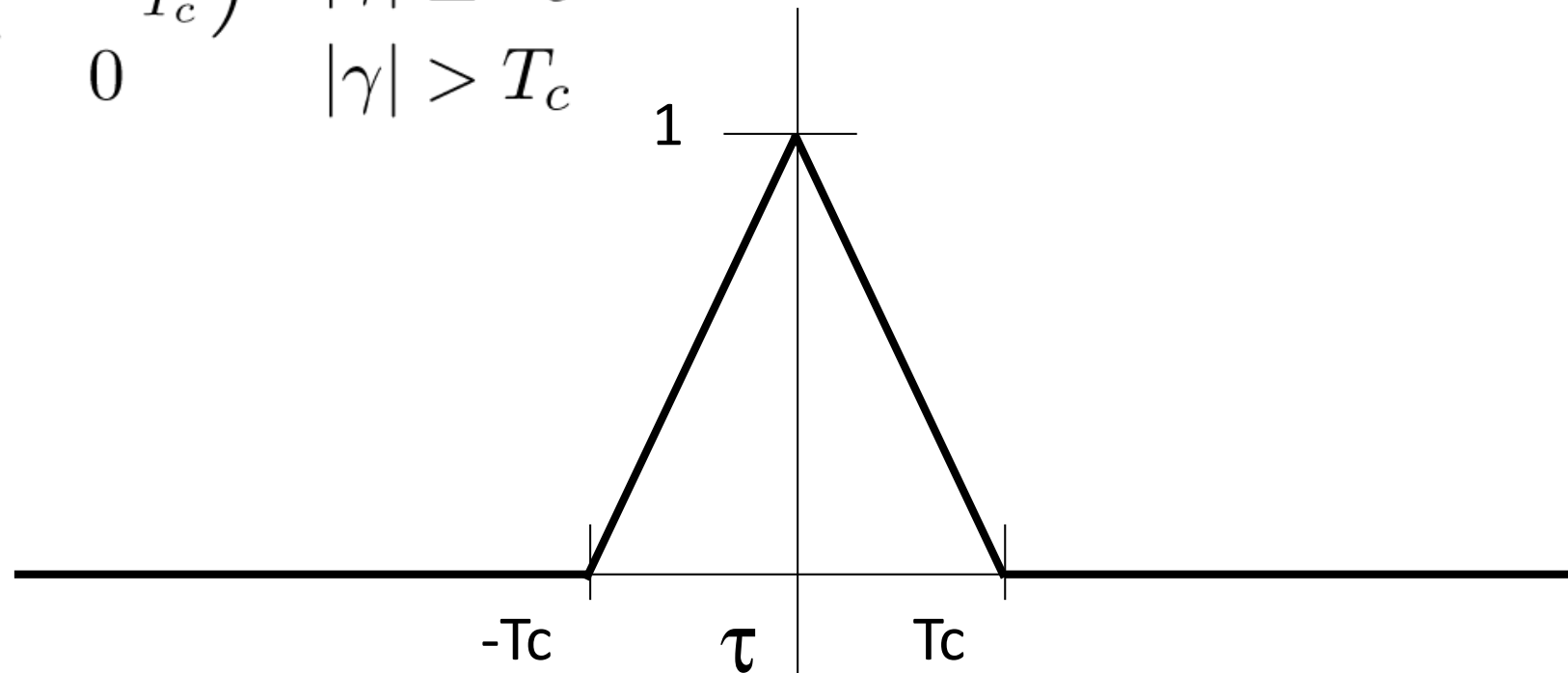
Multiplies it with received signal (red)

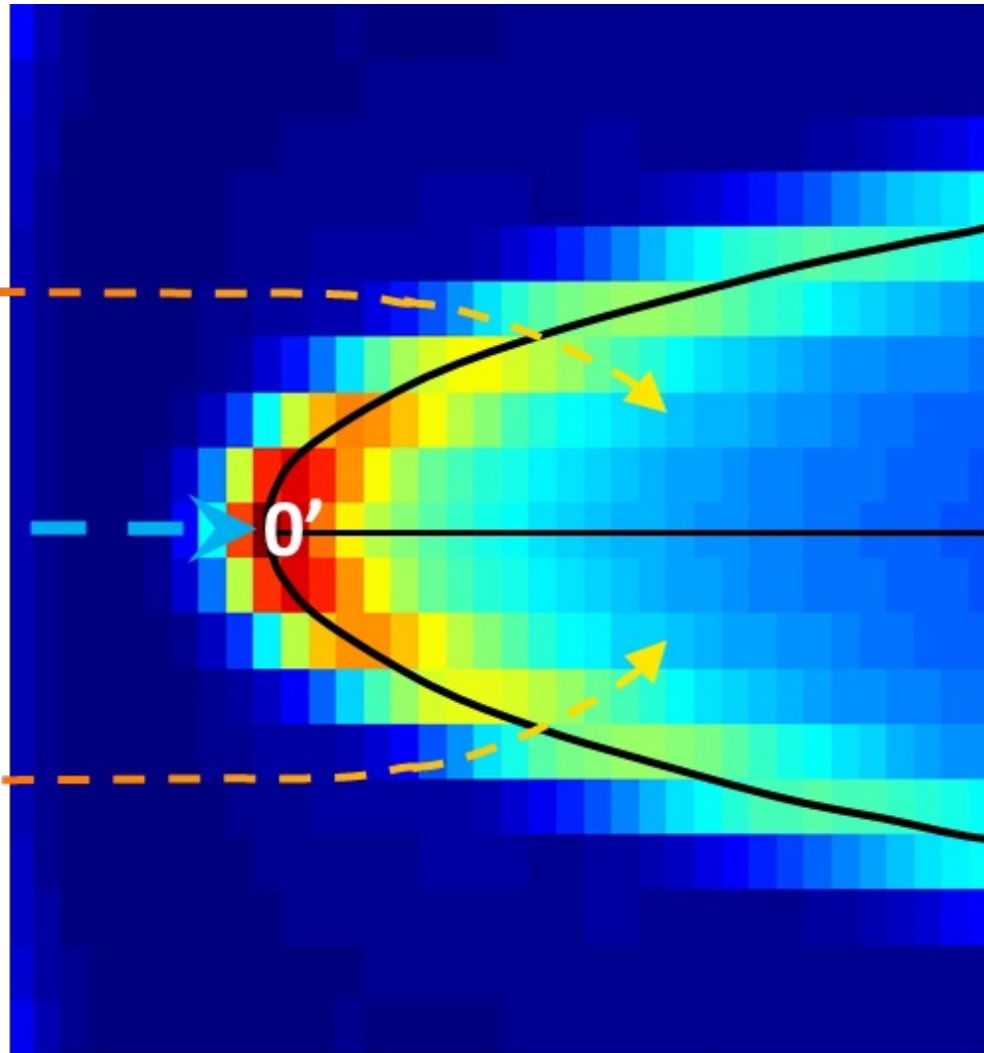


$$\tau = 0.05 T_c: \text{Sum} = 0.95(1) + 0.5(0) = \mathbf{0.95}$$

This is the mathematical process of *correlation*

$$R_s(\gamma) = \begin{cases} \left(1 - \frac{|\gamma|}{T_c}\right) & |\gamma| \leq T_c \\ 0 & |\gamma| > T_c \end{cases}$$



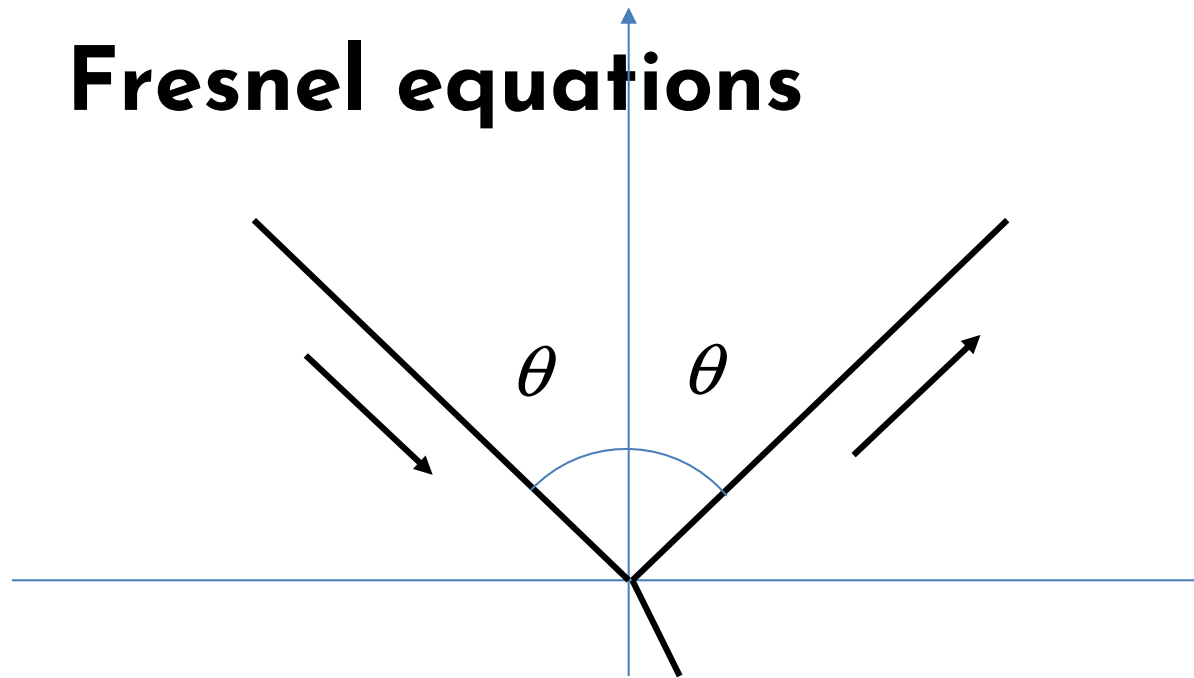


# From GNSS to GNSS+R





## Fresnel equations



$$\mathcal{R}_{HH} = \frac{\cos \theta - \sqrt{\epsilon_r - \sin^2 \theta}}{\cos \theta + \sqrt{\epsilon_r - \sin^2 \theta}}$$

$$\mathcal{R}_{VV} = \frac{\epsilon_r \cos \theta - \sqrt{\epsilon_r - \sin^2 \theta}}{\epsilon_r \cos \theta + \sqrt{\epsilon_r - \sin^2 \theta}},$$

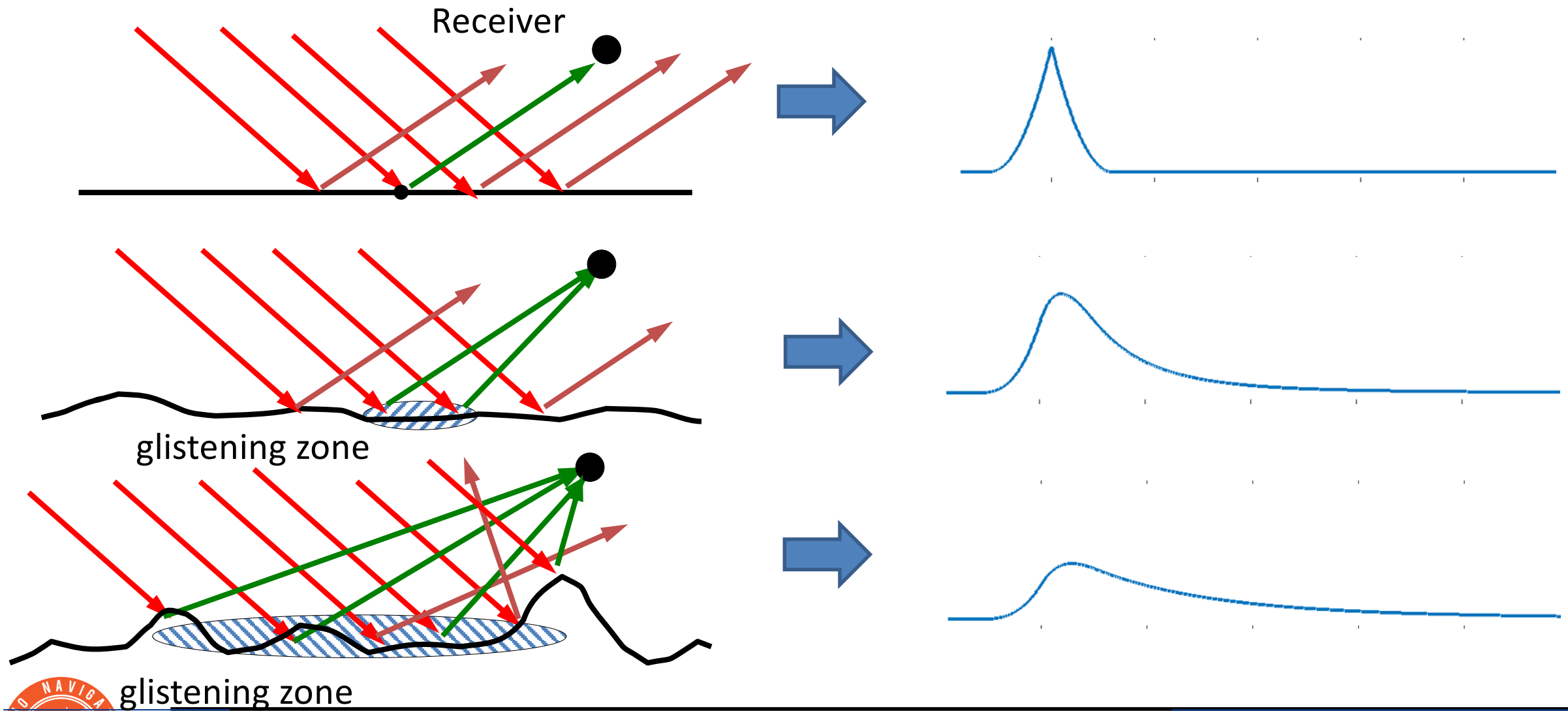
$$\begin{bmatrix} \mathcal{R}_{LL} & \mathcal{R}_{LR} \\ \mathcal{R}_{RL} & \mathcal{R}_{RR} \end{bmatrix} = \frac{1}{2} \begin{bmatrix} \mathcal{R}_{HH} + \mathcal{R}_{VV} & \mathcal{R}_{HH} - \mathcal{R}_{VV} \\ \mathcal{R}_{HH} - \mathcal{R}_{VV} & \mathcal{R}_{HH} + \mathcal{R}_{VV} \end{bmatrix}$$

## Dielectric constant ( $\epsilon_r$ ) function of surface properties:

- Land: Surface soil moisture, VWC, roughness (small)
- Ocean: Salinity (SSS), temperature (SST)



# Reflection from a rough surface



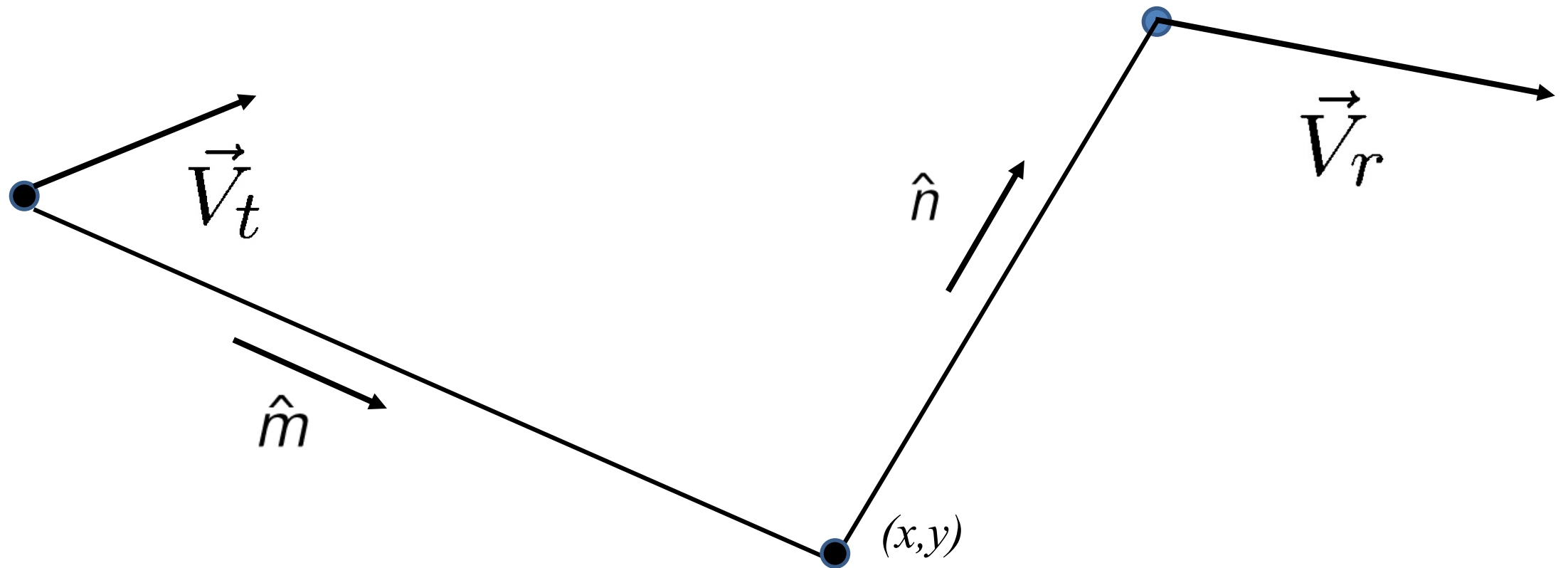
# Smooth (specular) vs rough (diffuse) scattering



(Photo taken 2020 Mays Lakes, Oak Brook, IL)



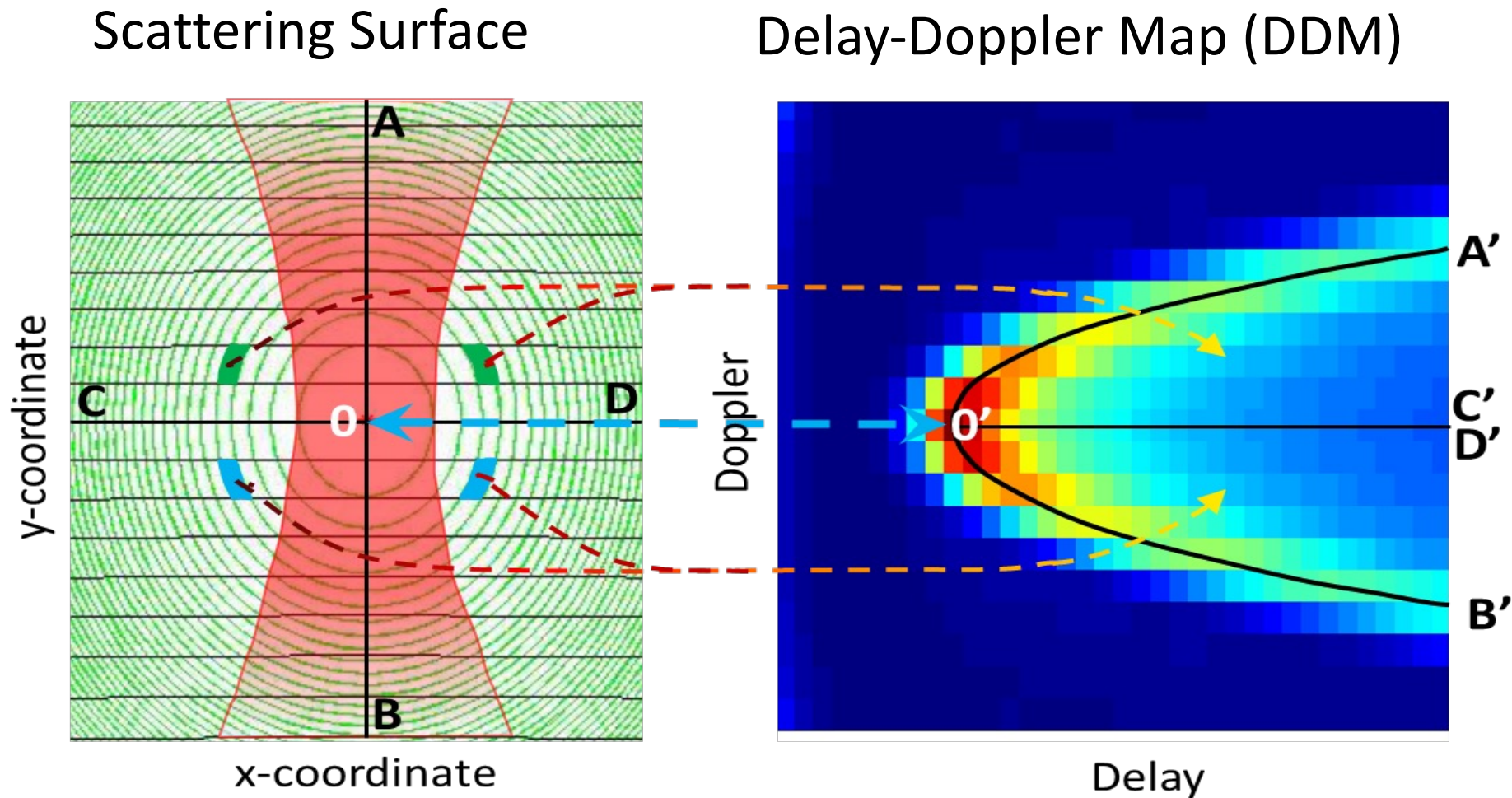
(Chapron and Ruffini, 2003 GNSS-R workshop, Barcelona. Photo taken at Le Conquet, Brittany)



$$f_D(x, y) = \frac{1}{\lambda} \left[ \vec{V}_t \cdot \hat{m}(x, y) - \vec{V}_r \cdot \hat{n}(x, y) \right]$$

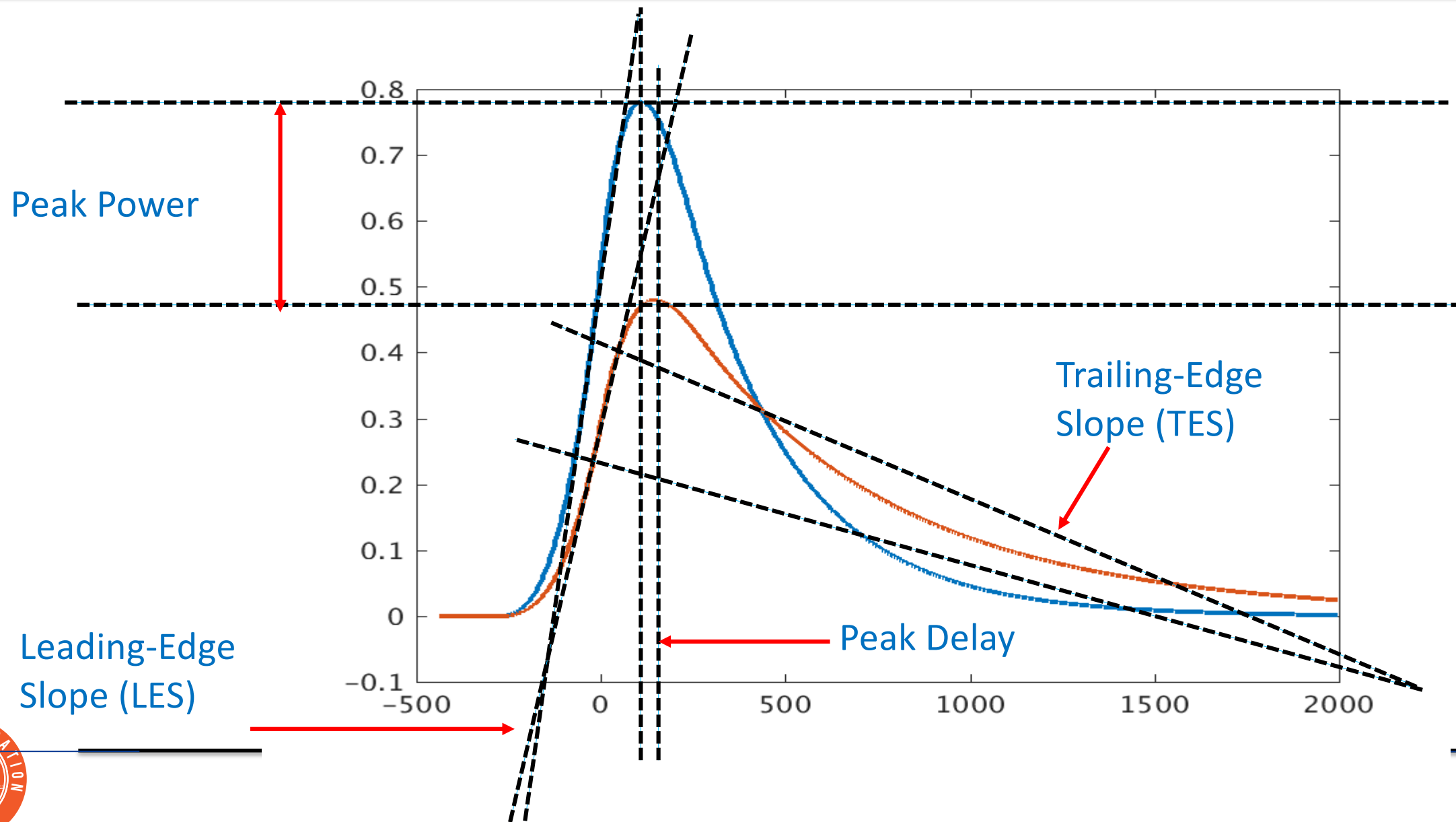


# Delay-Doppler Map (DDM)

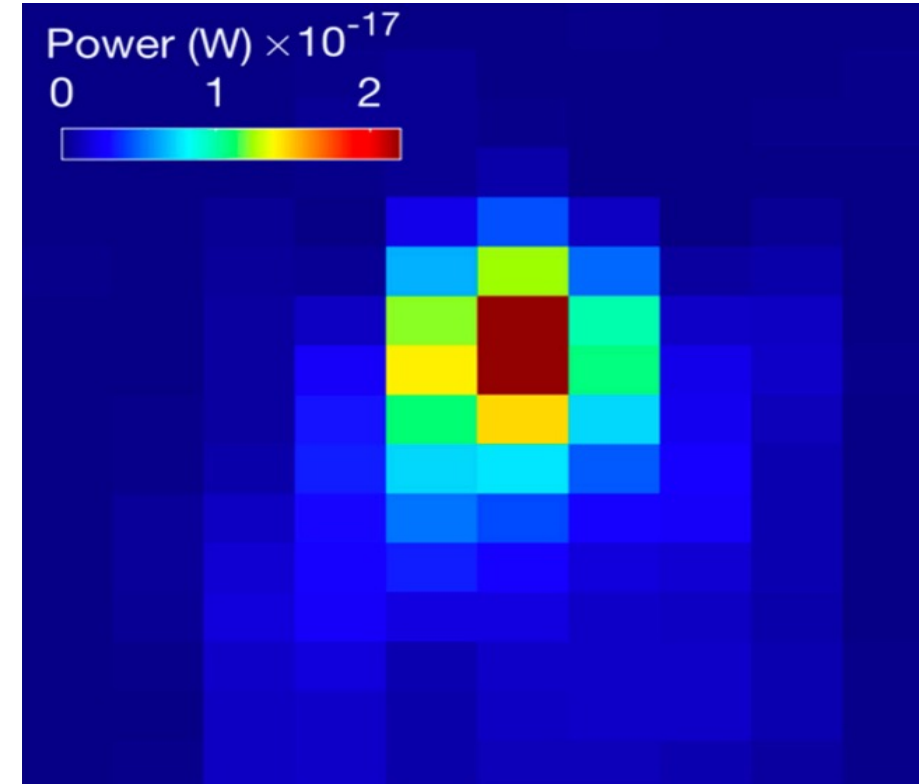


[Zavorotny, et al., IEEE GRSM DOI: 10.1109/MGRS.2014.2374220]

# Observables from the DDM



# Bistatic Radar Equation (BRE)





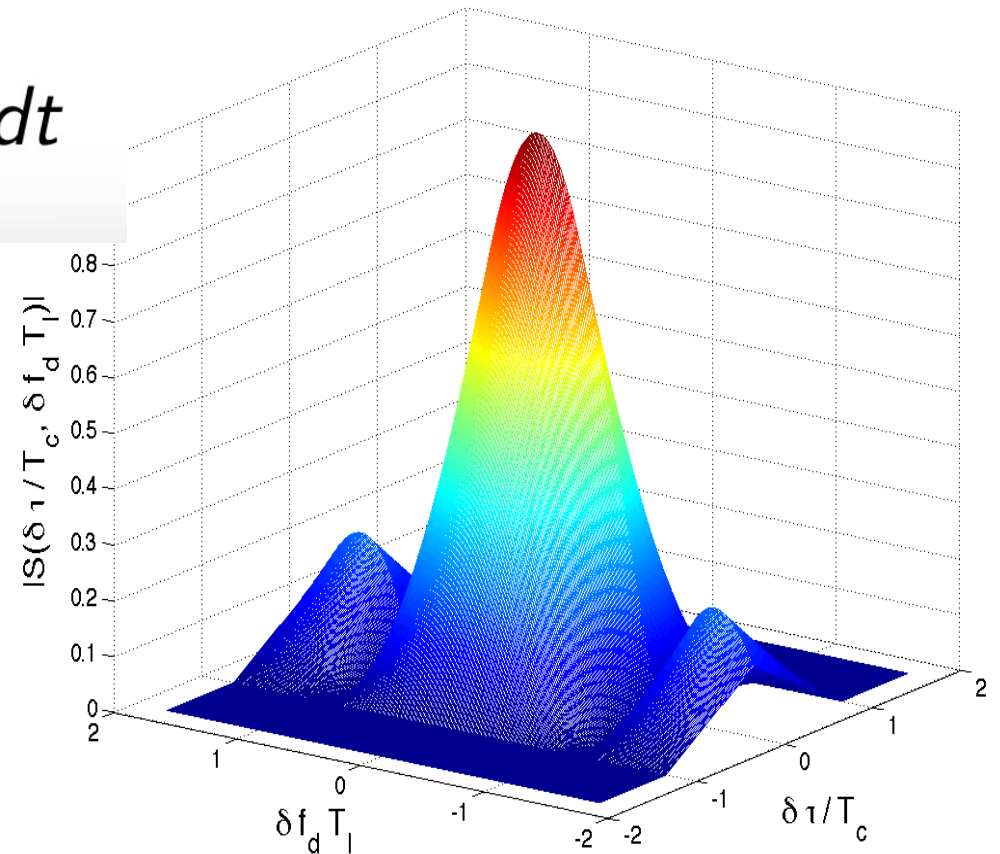
**Key part of navigation signal design**

$$\chi(\delta\tau, \delta f_D) = \frac{1}{T_I} \int s(t) s^*(t + \delta\tau) e^{-2\pi\delta f_D t} dt$$

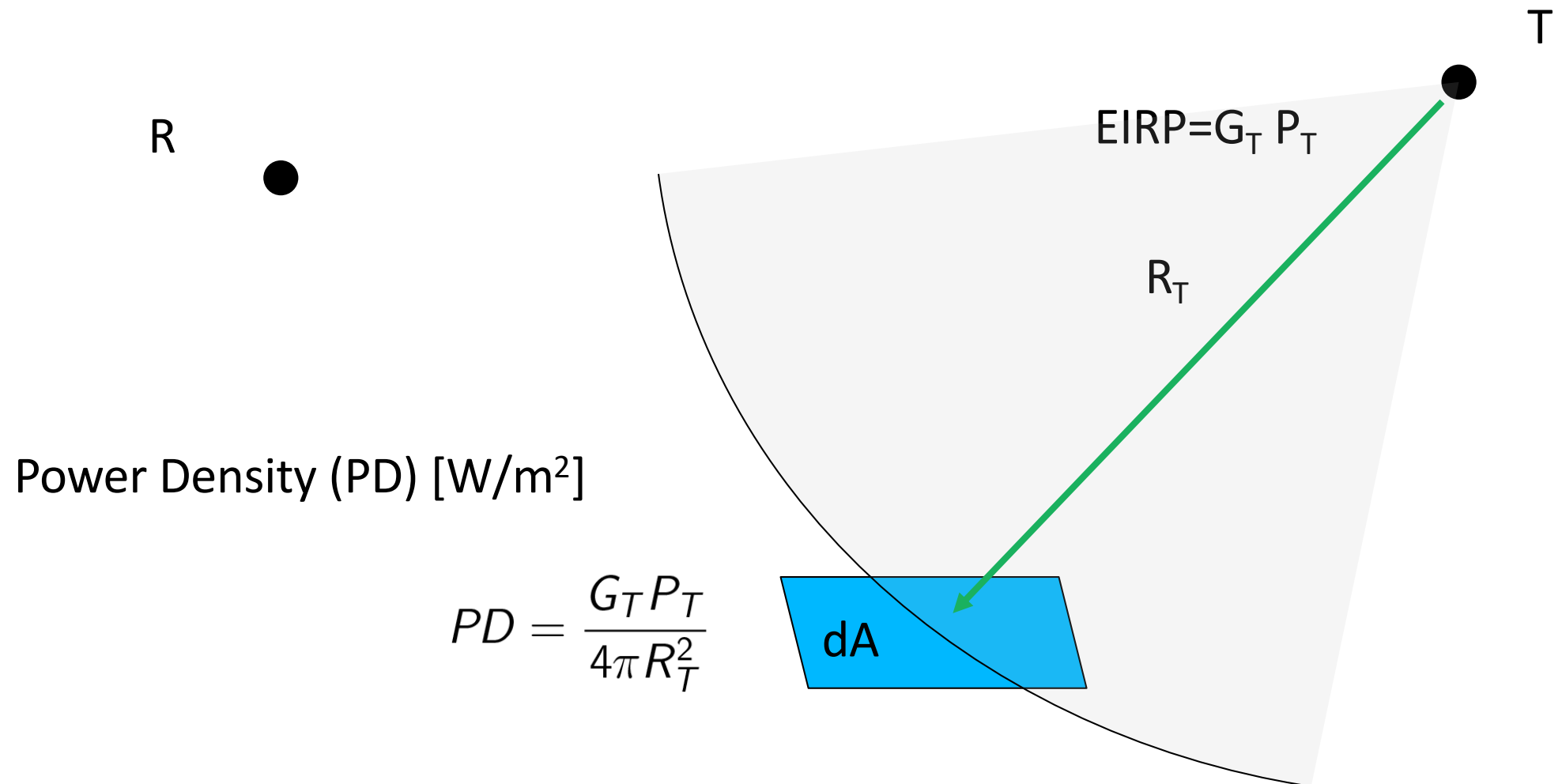
**Response of correlation to delay & Doppler error**

**First nulls (for BPSK signal):**

$$\delta\tau = \pm T_c \quad \delta f_D = \pm \frac{1}{T_I}$$



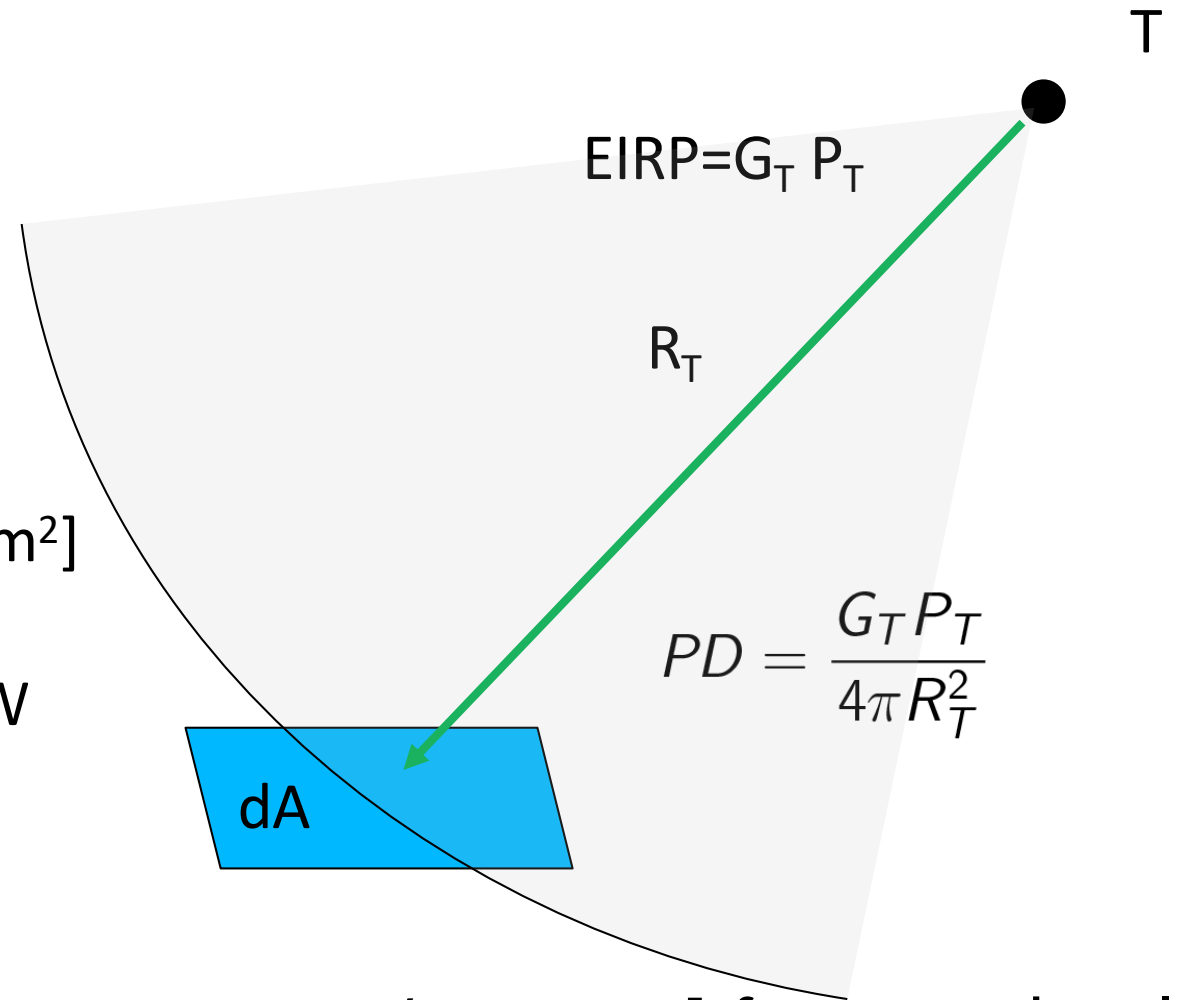
# Propagation for transmitter to surface



See [Zavorotny & Voronovich, TGARS, 2000,10.1109/36.841977] for more details

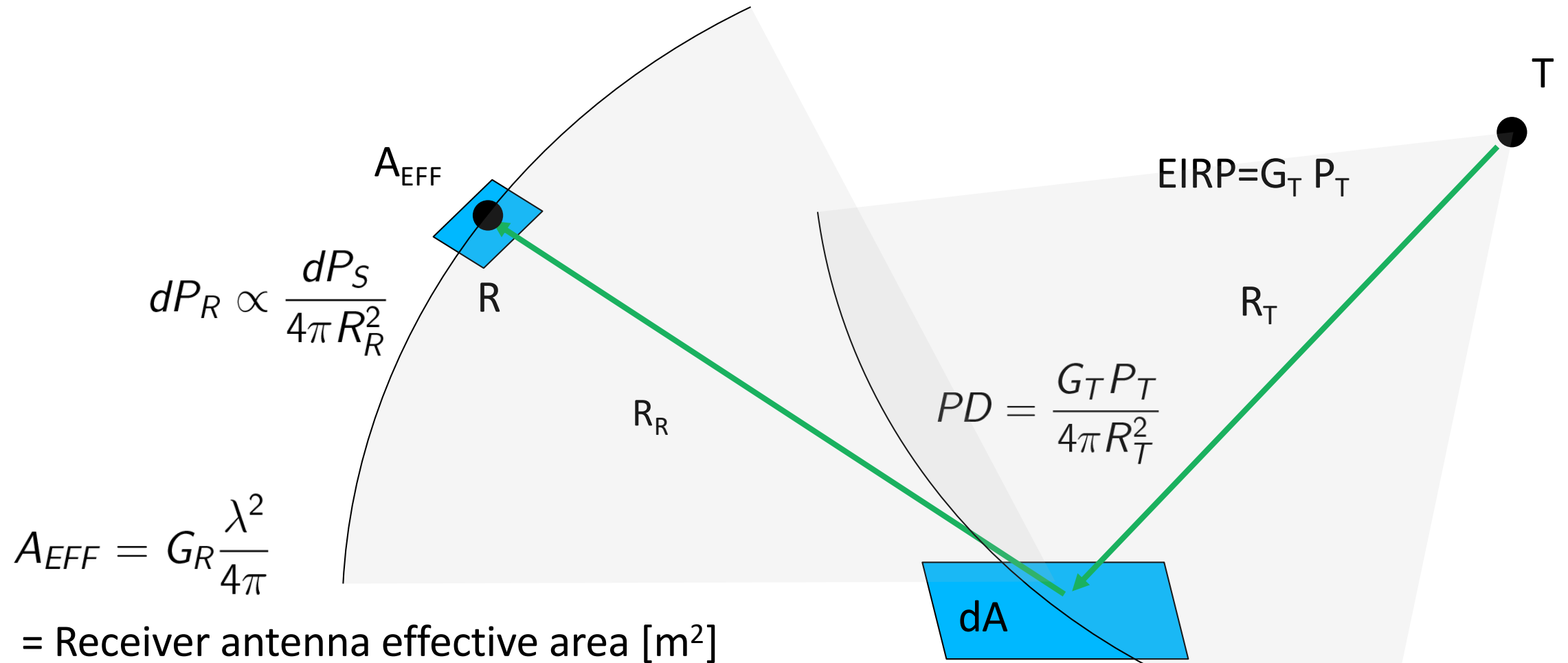
# Reflection from surface area dA

$\sigma^0$  = normalized bistatic cross-section [N.D.]  
 $\sigma^0 dA$  = Equivalent area of "perfect" reflector [m<sup>2</sup>]  
 $dP_S \propto \sigma^0 (PD) dA$  [W/m<sup>2</sup>] X [m<sup>2</sup>] = W



See [Zavorotny & Voronovich, TGARS, 2000,10.1109/36.841977] for more details

# Propagation from Surface to Receiver



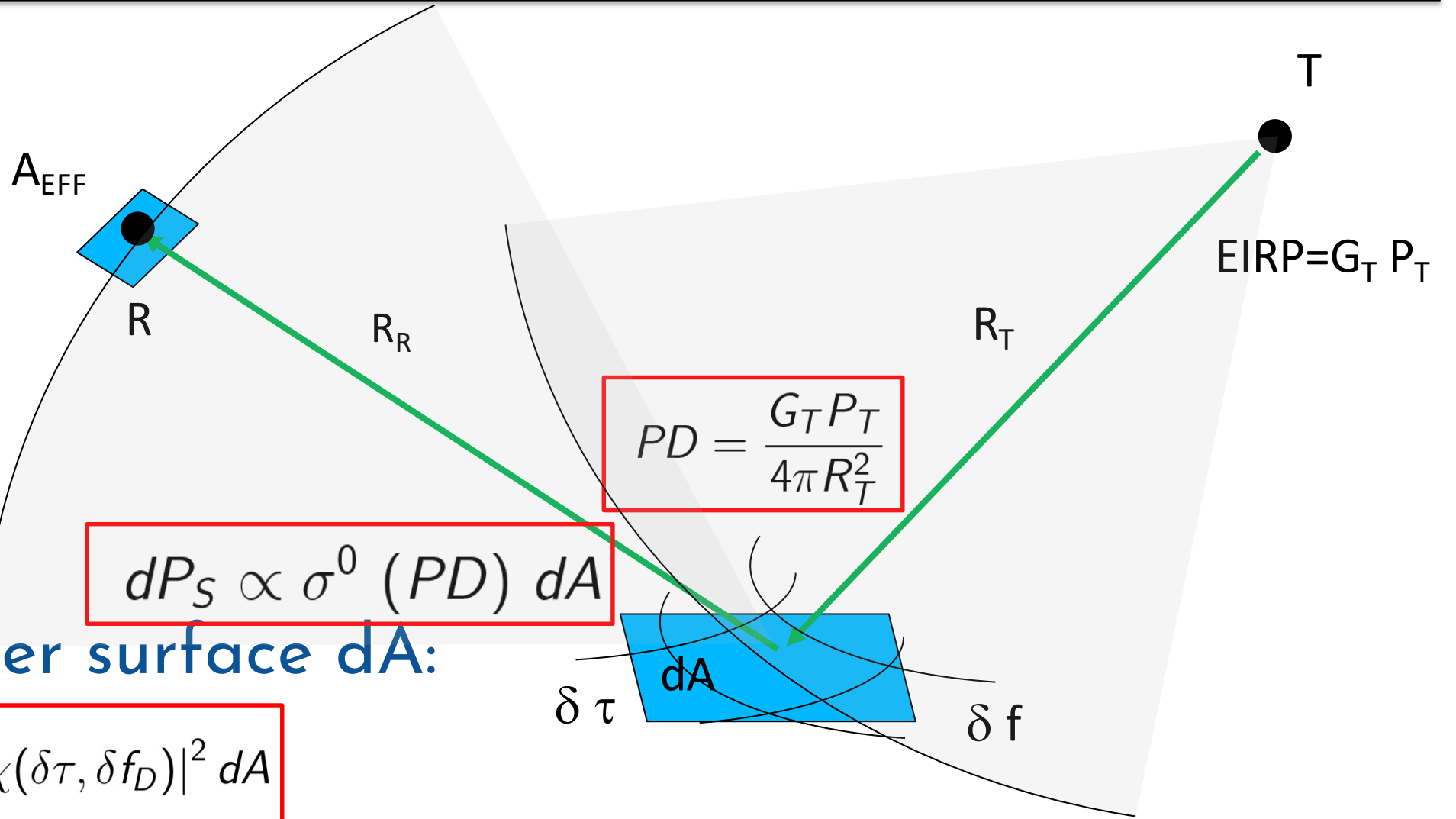
See [Zavorotny & Voronovich, TGARS, 2000,10.1109/36.841977] for more details



# Response of cross-correlation (WAF)

$$A_{EFF} = G_R \frac{\lambda^2}{4\pi}$$

$$dP_R \propto \frac{dP_S}{4\pi R_R^2}$$



$$PD = \frac{G_T P_T}{4\pi R_T^2}$$

$$dP_S \propto \sigma^0 (PD) dA$$

Integrate over surface  $dA$ :

$$P_R = \iint |\chi(\delta\tau, \delta f_D)|^2 dA$$

# Putting it all together ...

Integral over surface

$$P_R \propto \int |\chi(\delta\tau, \delta f_D)|^2 \times G_R \times \frac{1}{R_R^2} \times \sigma^0 \times \frac{1}{R_T^2} dA$$

Masking of  
Surface by  
delay-Doppler mapping

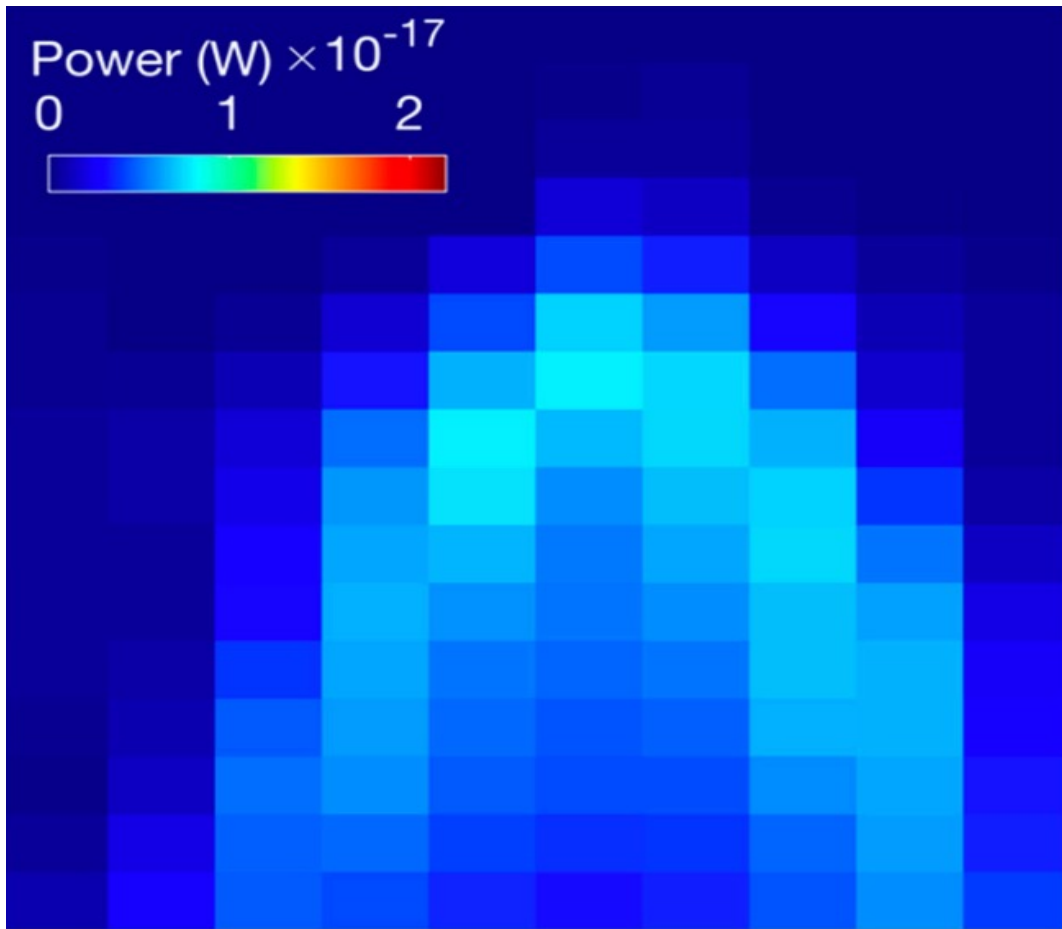
Masking of  
Surface by  
Receiver antenna

Path loss  
Surface-receiver

**Normalized  
Bistatic Radar  
Cross-section  
(NRBCS)**

Path loss  
Trans.-surface





## Delay Doppler Maps (DDM)



$$\langle |X(\tau, f)|^2 \rangle = \frac{\lambda^2 P_T G_T}{(4\pi)^3} \iint \frac{G_R |\chi(\Delta\tau, \Delta f)|^2}{R^2 R_0^2} \sigma_{pq}^0(\vec{\rho}) d^2\rho$$

## Random rough surface - DDM will be a random variable

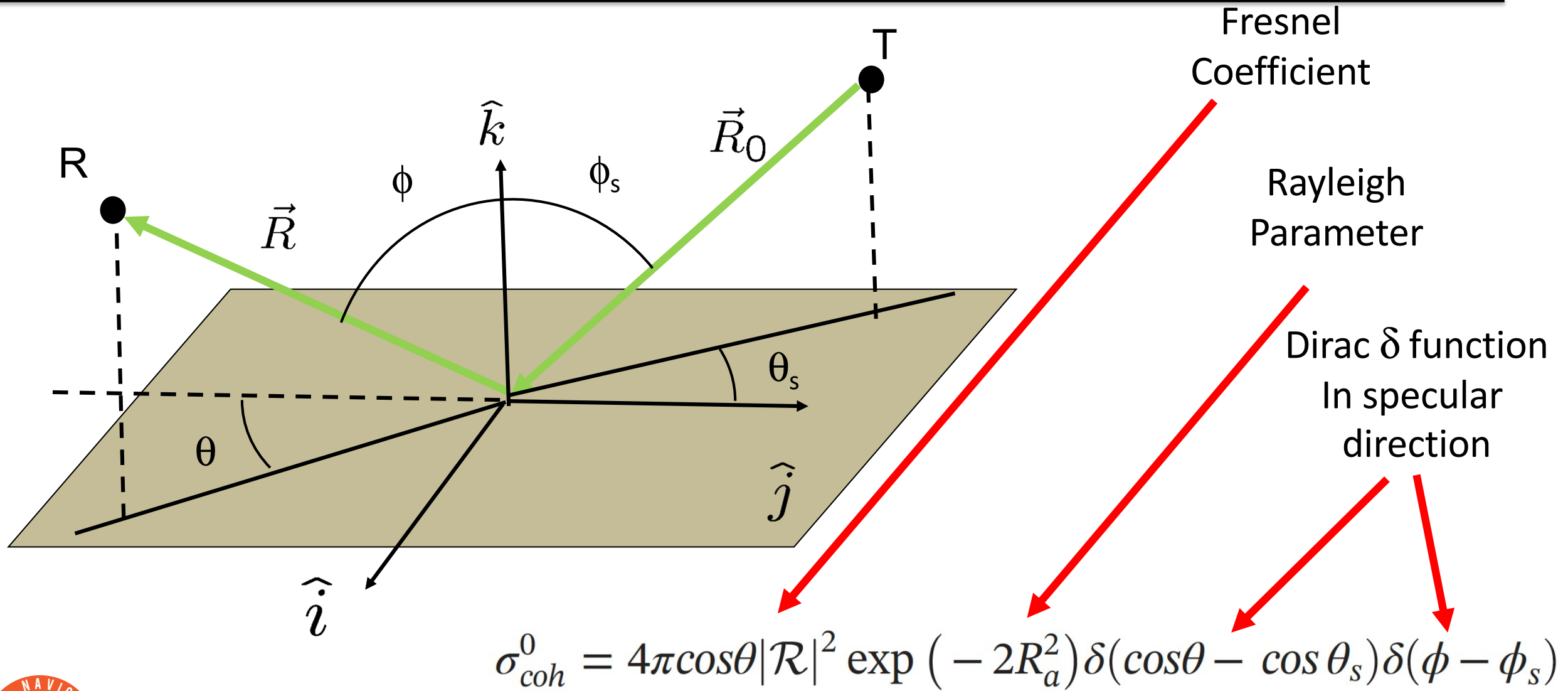
- Speckle
- Thermal noise
- $\langle \rangle$  is ensemble average (Expected value)

$\sigma_{pq}^0 =$  **NBRCS function of:**

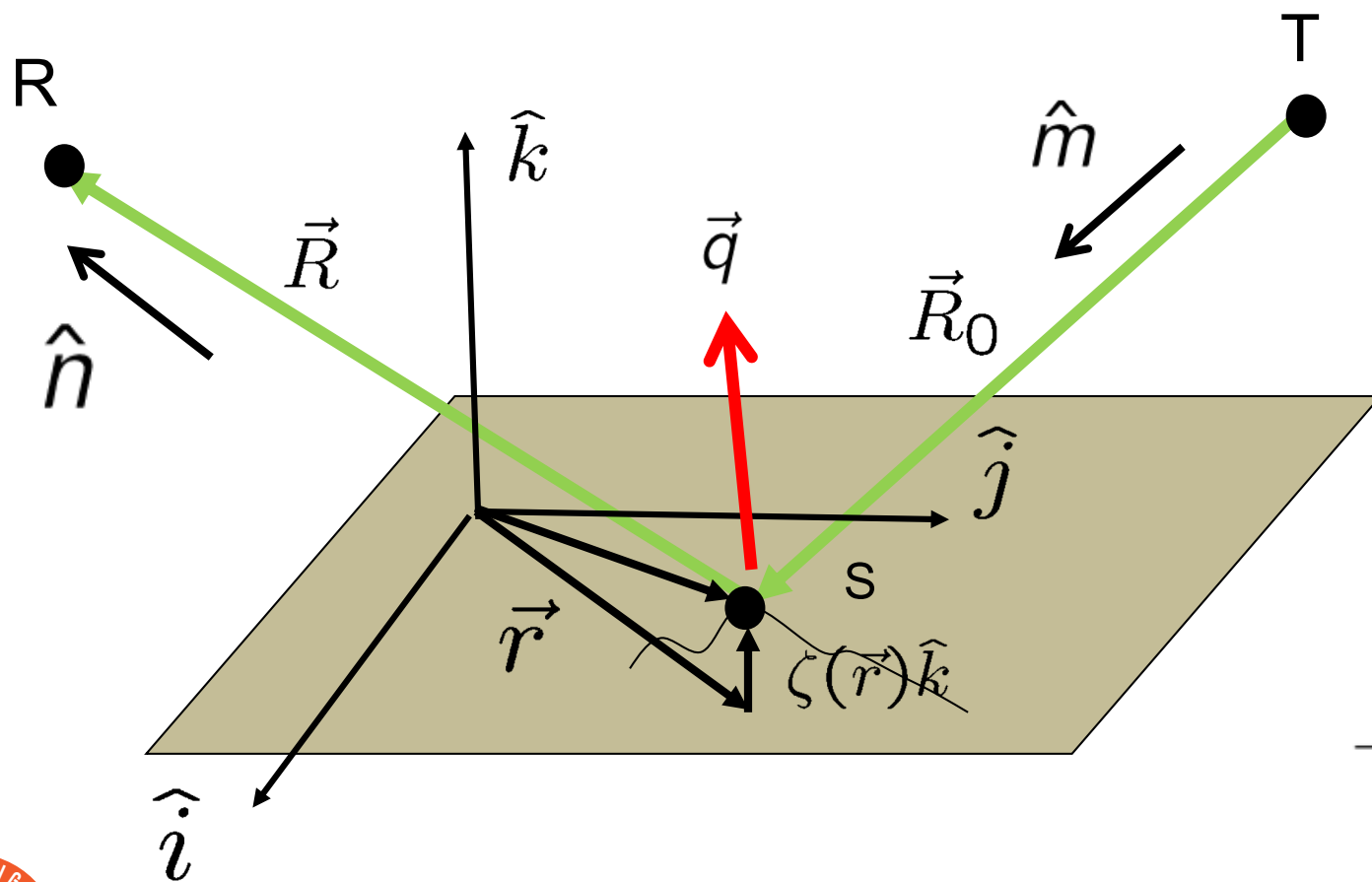
- Surface position ( $\vec{\rho}$ )
- Polarization (p,q)
- Surface roughness
- Reflectivity



# Specular (Coherent) Reflection



## Definition of the q-vector



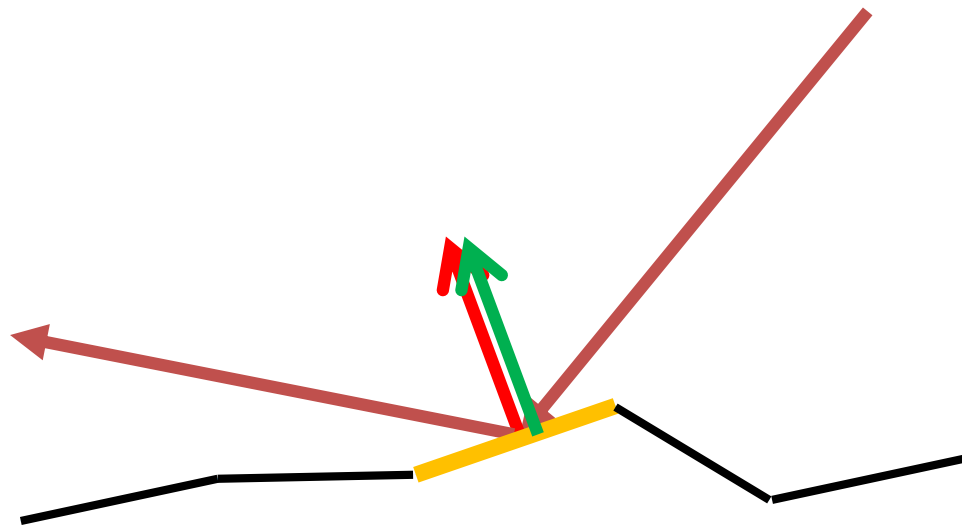
$$\vec{q} = \frac{2\pi}{\lambda}(\hat{m} - \hat{n})$$

$$\vec{q} = \vec{q}_\perp + q_z\hat{k}$$

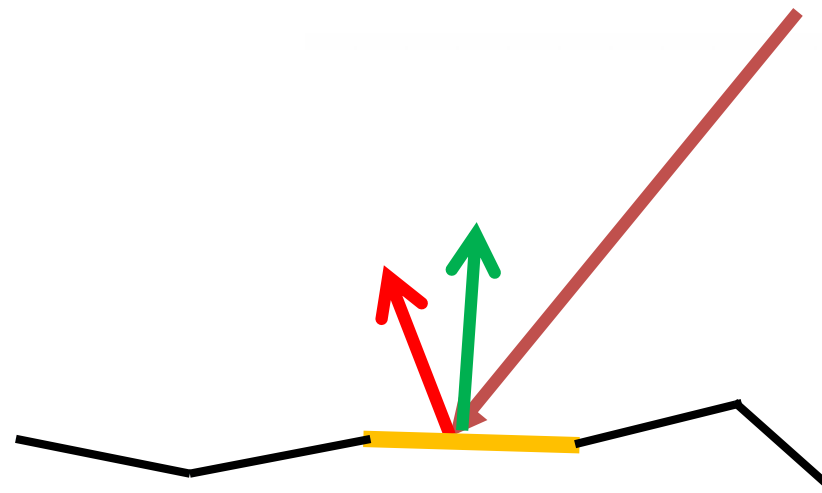
$$-\frac{\vec{q}_\perp}{q} = \text{bidirectional } \mathbf{Slope} \text{ of plane normal to } q$$

## NBRCS proportional to slope PDF Physical interpretation:

$$\sigma^0 = \pi |\mathfrak{R}|^2 \left( \frac{q}{q_z} \right)^4 P_{\vec{v}} \left( -\frac{\vec{q}_{\perp}}{q_z} \right),$$



Probability of surface slope  
Giving "specular" reflection  
In direction of receiver



Green = normal to surface  
Red = bisector (q) vector

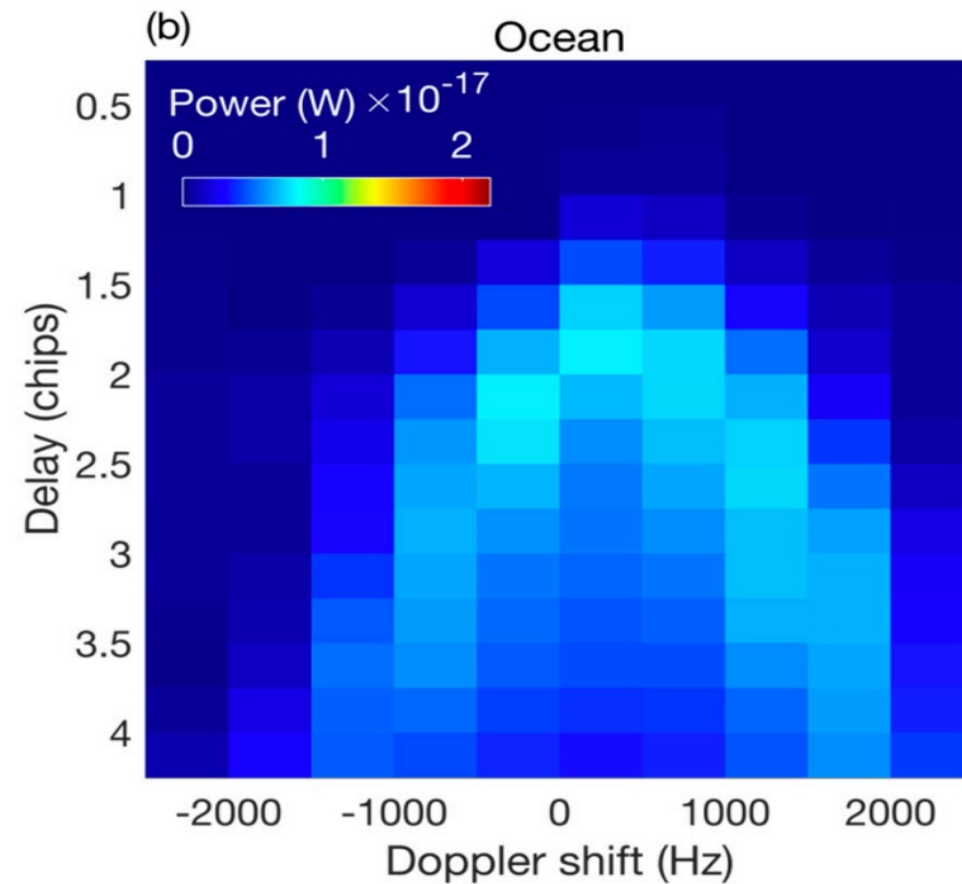
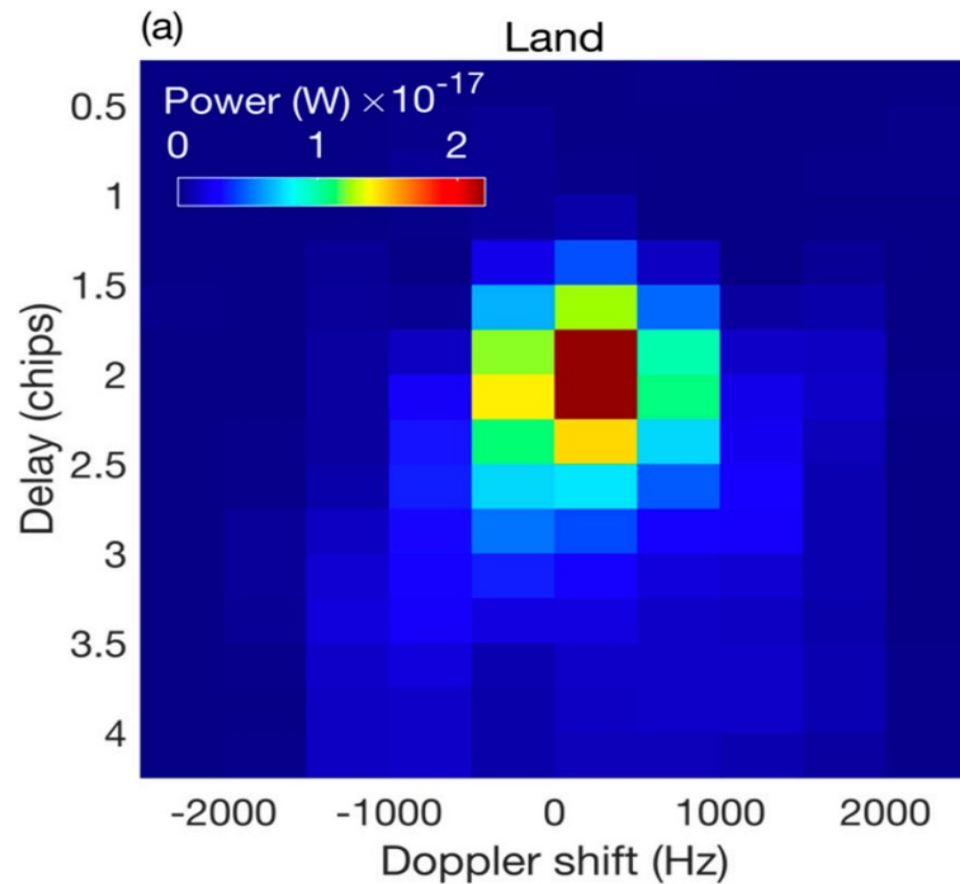
[Barrick, Proc. IEEE, 1968, 10.1109/PROC.1968.6718]

# Coherent

# Incoherent

$$\langle |Y(\tau_s, f_s)|^2 \rangle = \frac{\lambda^2 P_T G_T}{(4\pi)^2} \frac{G_R}{(R + R_0)^2} \Gamma$$

$$\langle |X(\tau, f)|^2 \rangle = \frac{\lambda^2 P_T G_T}{(4\pi)^3} \iint \frac{G_R |\chi(\Delta\tau, \Delta f)|^2}{R^2 R_0^2} \sigma_{pq}^0(\vec{\rho}) d^2\rho$$

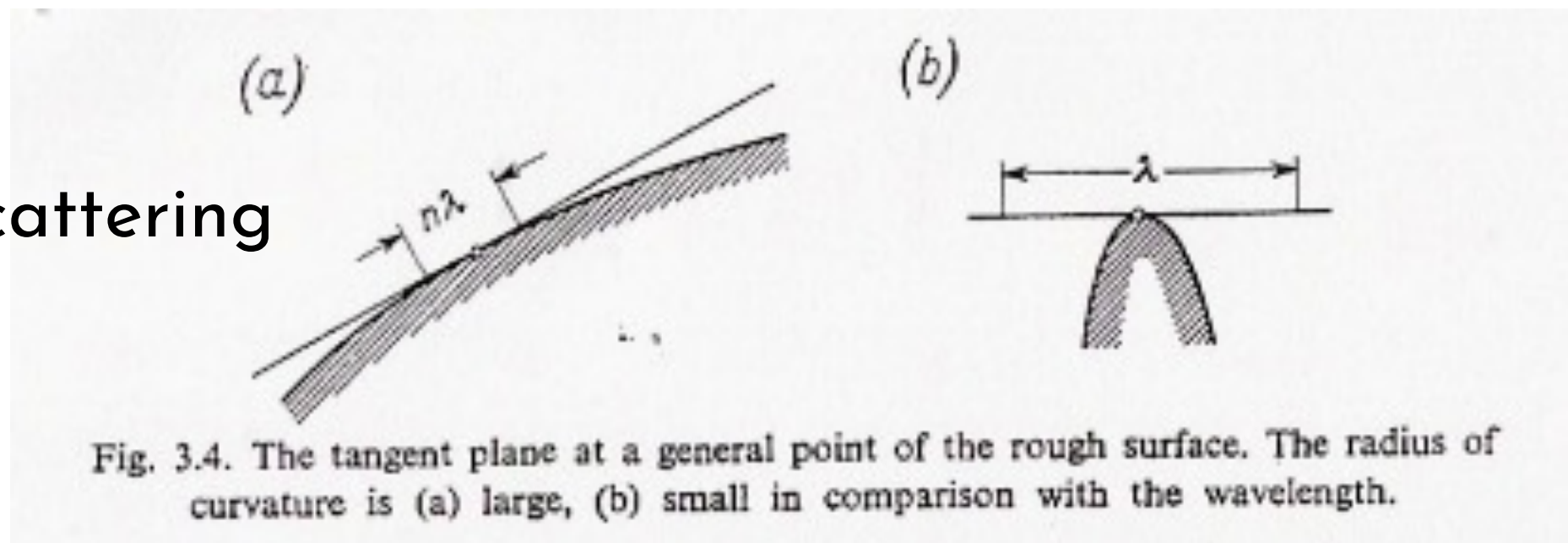


## Kirchoff Approximation - Geometric Optics (KA-GO):

- Local radius of curvature  $\gg$  Wavelength
- Far field:  $k \gg 1/R, 1/R_0$

### Limitations:

- Depolarization
- Out of plane scattering



[Beckmann & Spizzichino, 1987]

## **Kirchhoff Approximation (Physical Optics)**

[Elfouhaily & Guérin (2004), 10.1088/0959 7174/14/4/R01]

[De Roo & Ulaby (1994) 10.1109/8.277216]

## **Small Perturbation Method (SPM) - small surface variations & slopes**

## **Two-Scale Model - early attempt to unify KA & SPM - arbitrary dividing wavenumber**

[Bass & Fuks (1979) Wave Scatt. from Stat. Rough Surfaces]

[Valenzuela (1978) 10.1007/BF00913863]

[Brown (1978) 10.1109/TAP.1978.1141854]





**Integral Equation Models** - computationally expensive - reduces to GO for high frequency and SPM for low frequencies

**Small-Slope Approximation** - a “unifying method” - integrates entire spectrum without splitting into large & small scale - popular in GNSS-R

[Voronovich (2013) Wave Scattering from Rough Surfaces]



# Calibration



[Wang, et al., 10.1109/JSTARS.2018.2867773]

## Direct signal used to calibrate receiver gains

[Egido, et al. Remote Sensing (2012),10.3390/rs4082356]

- Correlator output in counts:  $C(\tau, f)$
- “Through” (T) configuration

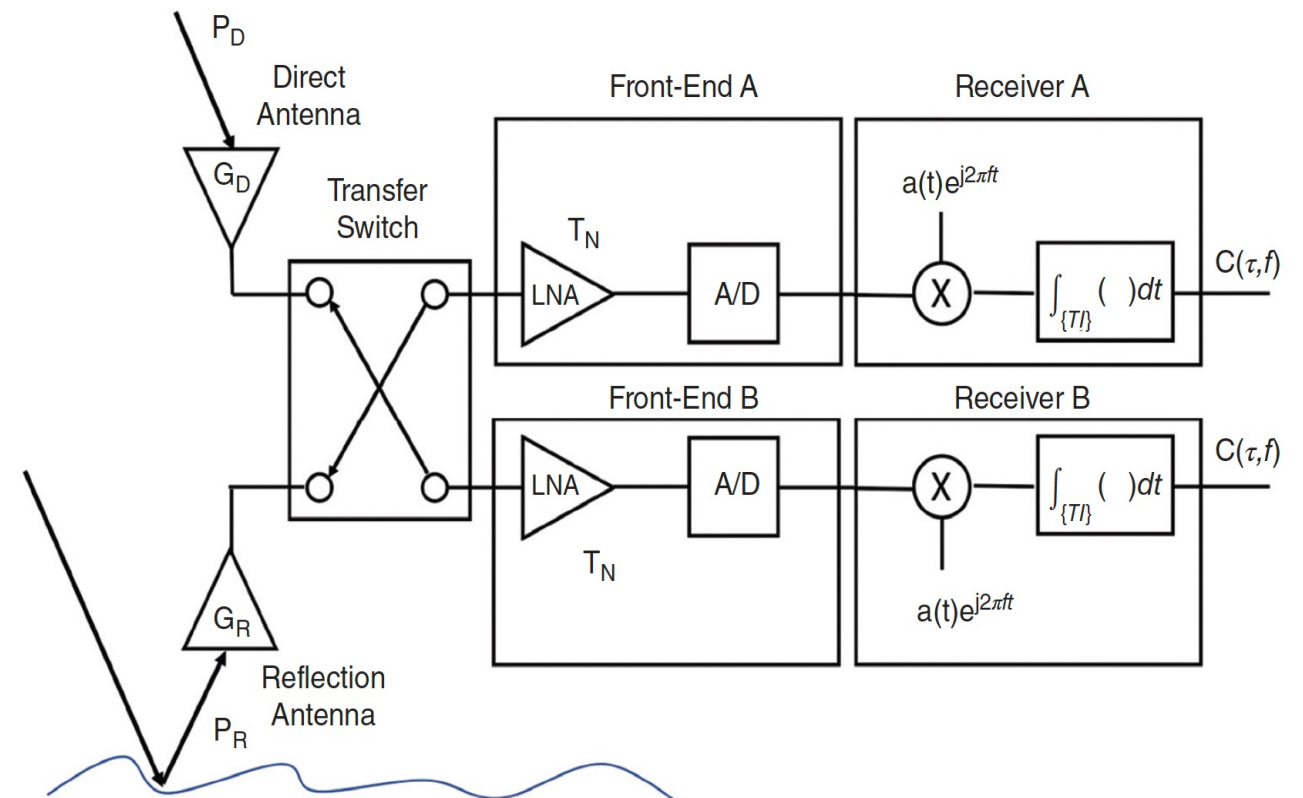
$$\frac{P_R}{P_D} = \left(\frac{G_A}{G_B}\right) \left(\frac{G_D}{G_R}\right) \frac{C_B^T - C_{N,B}^T}{C_A^T - C_{N,A}^T}$$

- “Swap (S) configuration

$$\frac{P_R}{P_D} = \left(\frac{G_B}{G_A}\right) \left(\frac{G_D}{G_R}\right) \frac{C_A^S - C_{N,A}^S}{C_B^S - C_{N,B}^S}$$

- These can be combined to cancel the receiver gain ratio

$$\frac{G_A}{G_B} = \frac{C_A^T - C_{N,A}^T}{C_B^S - C_{N,B}^S}$$



[PNT in 21<sup>st</sup> Century (10.1002/9781119458449.ch34)]

## Level 1a: DDM in calibrated power (units of W)

- Method Follows the CYGNSS ATBD
- Uses calibration source in receiver @  $T_B$

$$C_B = G(P_B + P_{N,I})$$

- $G$  = Receiver gain (unknown)
- $P_{N,I}$  = Receiver noise power, calibrated with  $T_R$

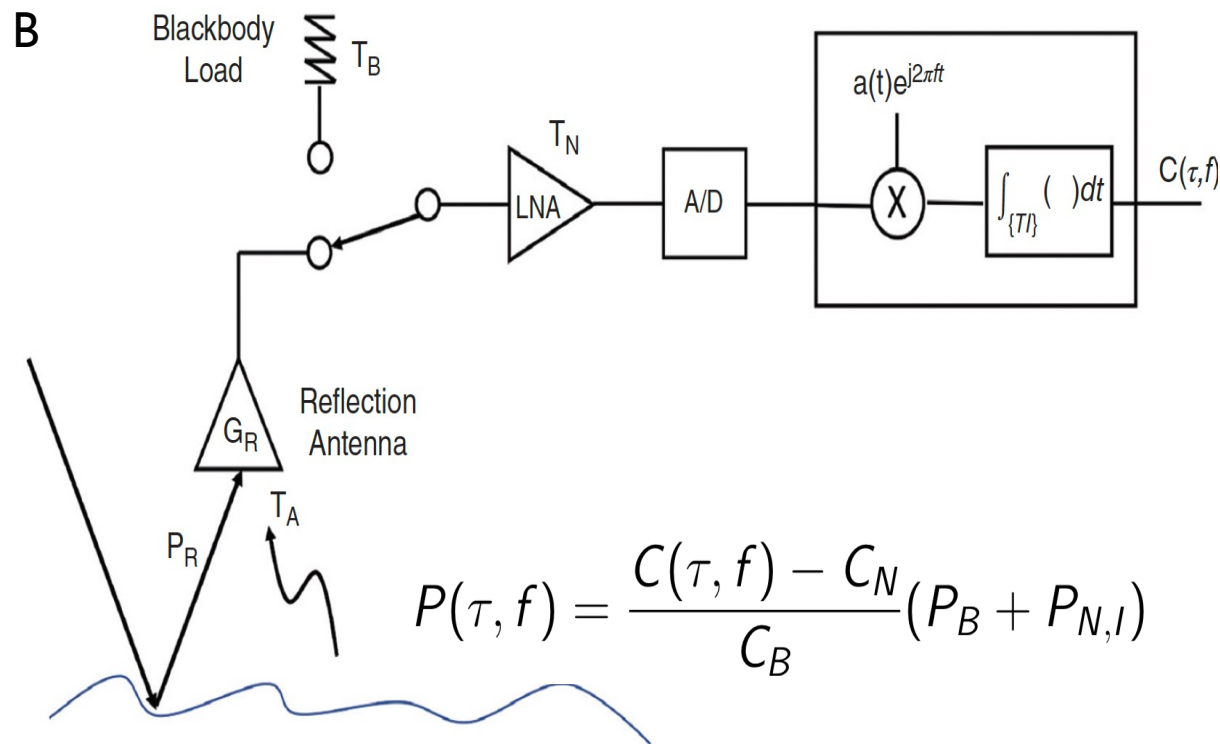
$$P_{N,I} = kB_I(290K)(NF(T_R) - 1)$$

- DDM in counts given by:

$$C(\tau, f) - C_N = GP(\tau, f)$$

$C_N$  = counts in noise-only

“forbidden zone” of DDM

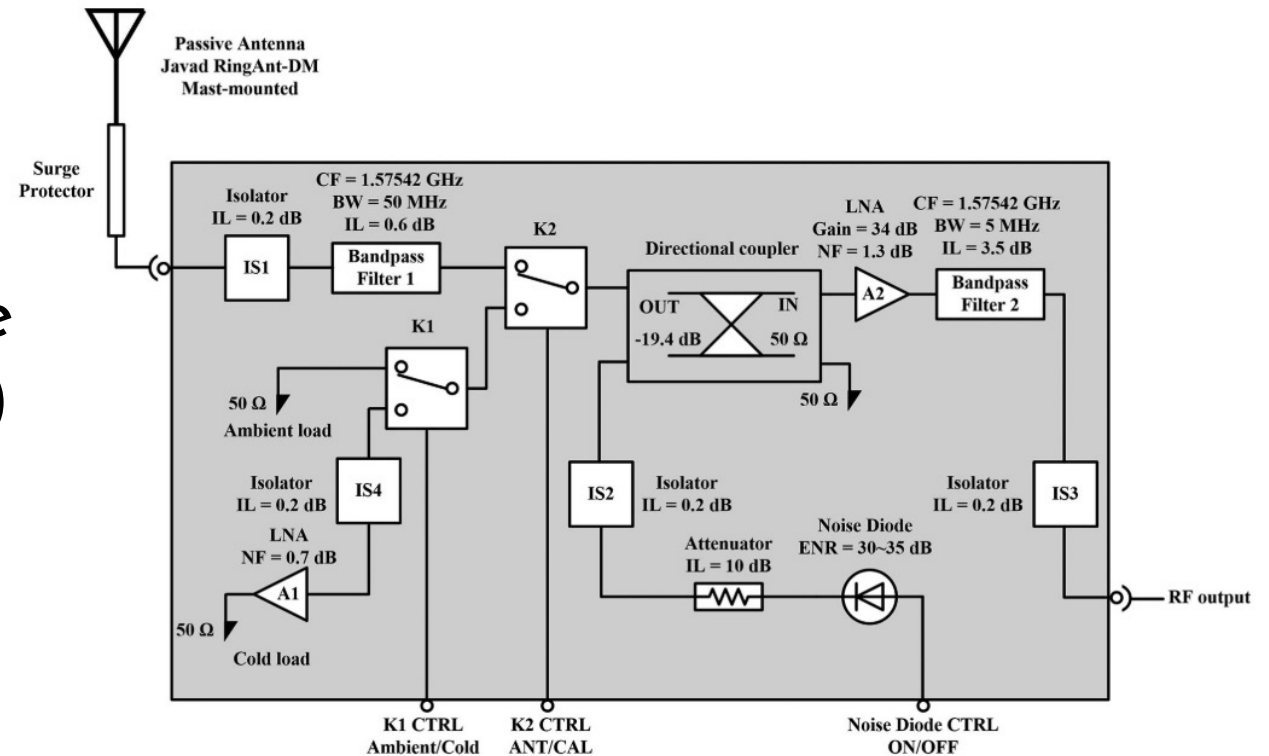


$$P(\tau, f) = \frac{C(\tau, f) - C_N}{C_B} (P_B + P_{N,I})$$

[PNT in 21<sup>st</sup> Century (10.1002/9781119458449.ch34)]

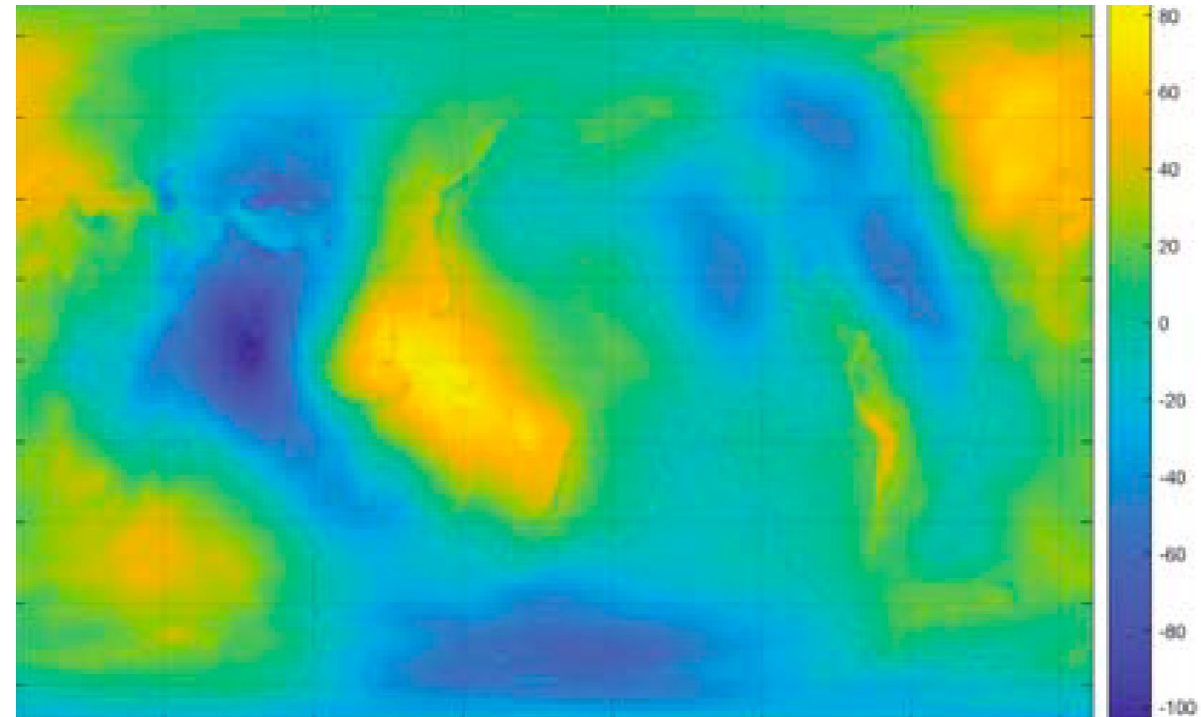
## Source power and antenna gain estimates

- DDM calibration of requires:
  - Transmitter power
  - Transmitter gain patterns
- GPS satellites can adaptively allocate power between channels (Flex power)
- Ground-based system designed at Michigan for support of CYGNSS
- Augmented by on-board power monitoring using direct antenna



[Wang, et al., 10.1109/JSTARS.2018.2867773]

# Delay-Doppler Geometry

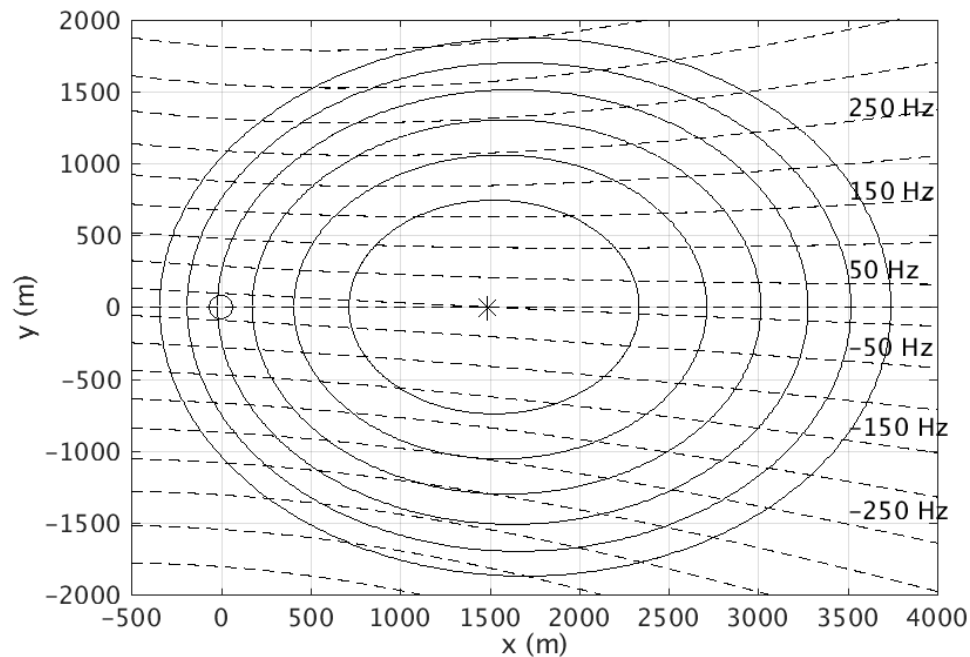




**Iso-range:**  $\rho(x, y) = |\vec{R}_T - \vec{R}_S(x, y)| + |\vec{R}_R - \vec{R}_S(x, y)|$

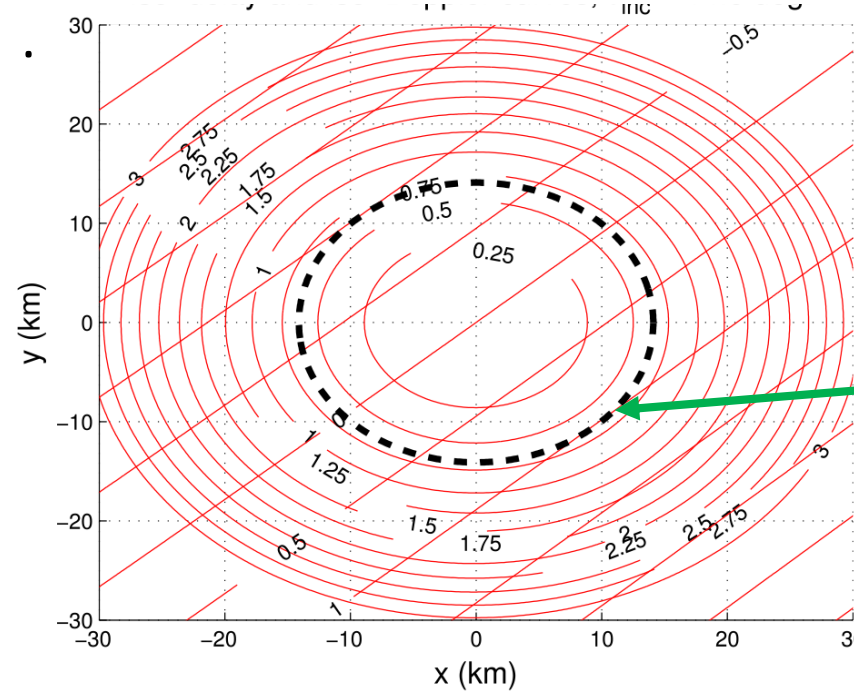
**Iso-Doppler:**  $f_D(x, y) = \frac{1}{\lambda} [\vec{V}_t \cdot \hat{m}(x, y) - \vec{V}_r \cdot \hat{n}(x, y)]$

Airborne Receiver 4.6 km altitude



1/4 chip delay  
increment

Satellite Receiver 500 km altitude



25 km  
Resolution





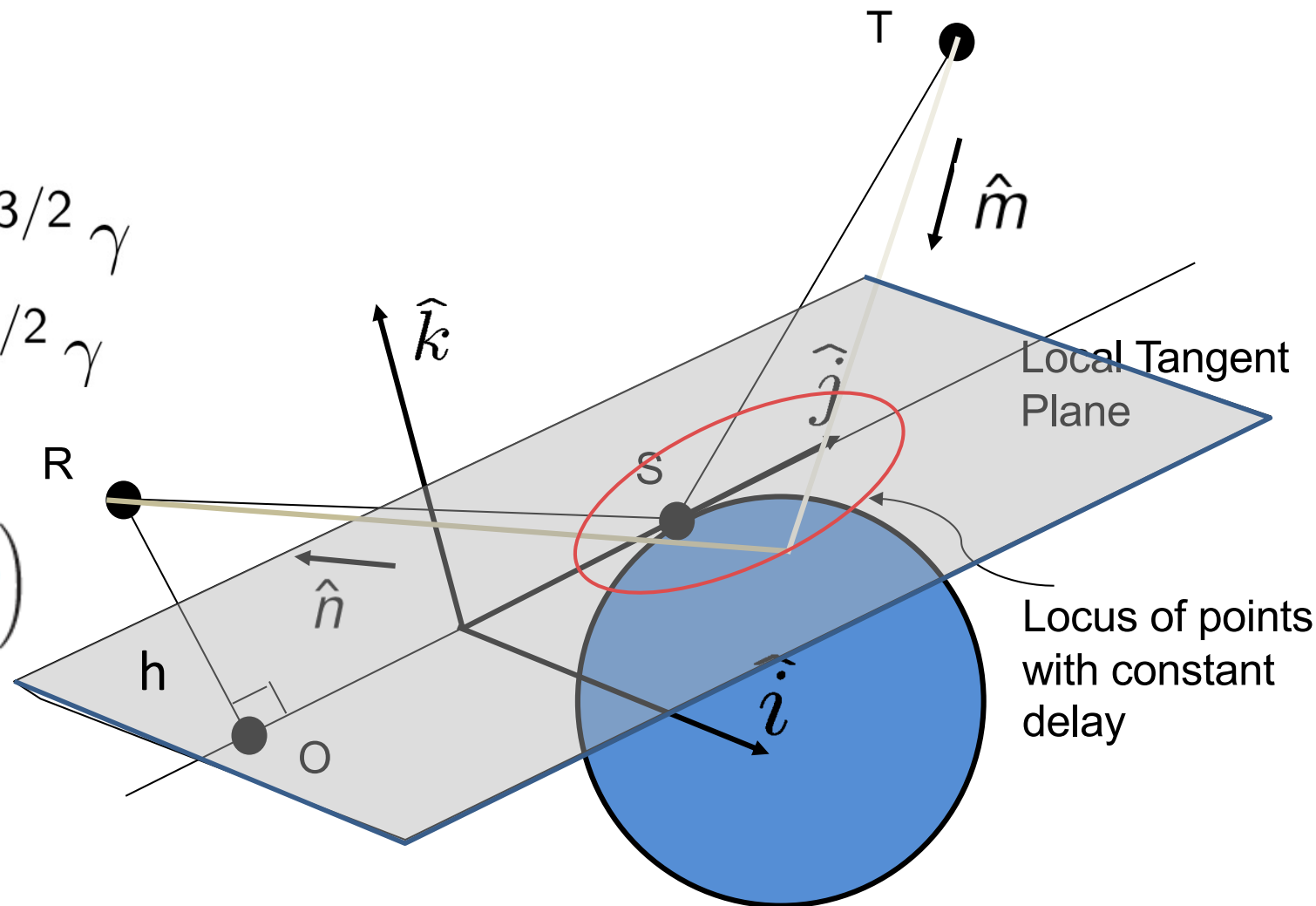
**Iso-range ellipse :**

$$a \approx \sqrt{2ch\tau} \sin^{-3/2} \gamma$$

$$b \approx \sqrt{2ch\tau} \sin^{-1/2} \gamma$$

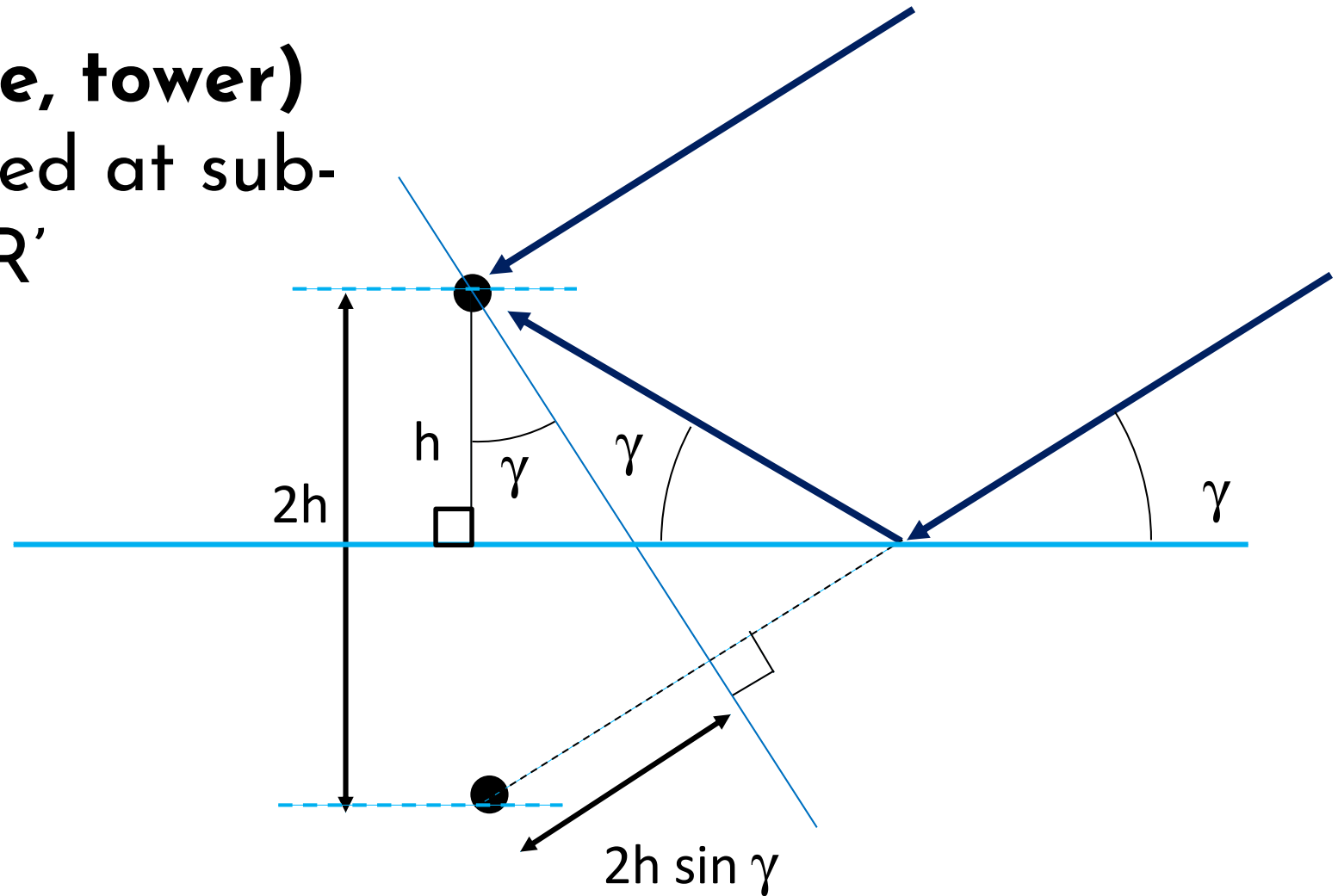
**Iso-Doppler hyperbola:**

$$(x_0, y_0) = \left( \frac{hV_x V_z}{V_x^2 + V_y^2 - V_D^2}, \frac{hV_y V_z}{V_x^2 + V_y^2 - V_D^2} - h \tan \theta \right)$$



**Low-altitude (airborne, tower)**  
 Reflected signal received at sub-  
 surface "virtual point" R'

$$c\tau_s = 2h \sin \gamma$$

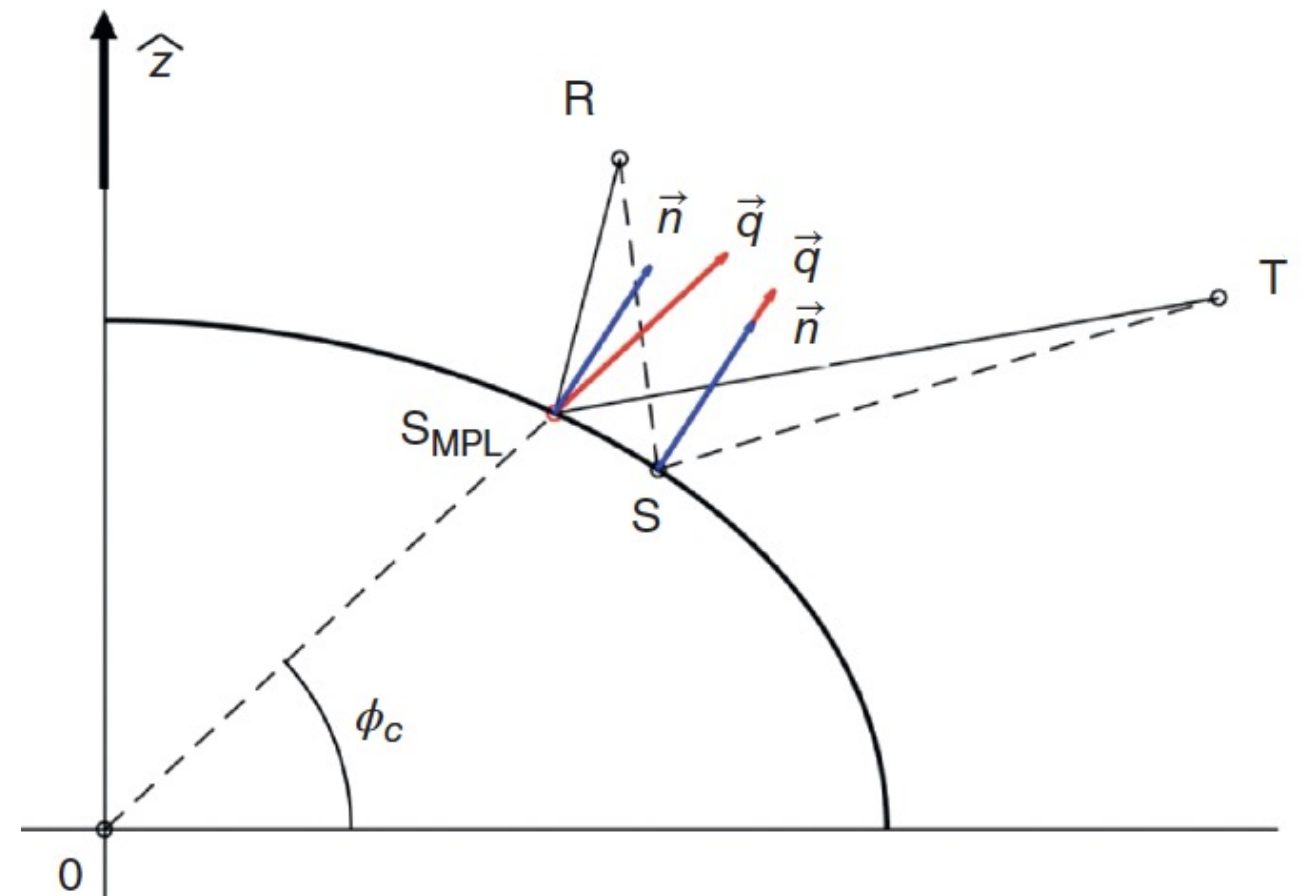


**Fermat's principle**  
(Minimum path delay)

$$\rho(\vec{R}_S) = |\vec{R}_T - \vec{R}_S| + |\vec{R}_R - \vec{R}_S|$$

**Snell's Law ( $\theta_I = \theta_R$ )**  
(bisector  $\vec{q}$  aligned with surface normal  $\vec{n}$ )

**Can be refined further in post-process**



[PNT in 21<sup>st</sup> Century (10.1002/9781119458449.ch34)]

## Unconstrained optimization ( $\vec{R}_S(\phi, \lambda)$ is eqn. of ellipsoid)

Minimize:  $J_{unc}(\phi, \lambda) = \left| \vec{R}_T - \vec{R}_S(\phi, \lambda) \right| + \left| \vec{R}_R - \vec{R}_S(\phi, \lambda) \right|,$

## Constrained optimization

Minimize:  $J_{MPL}(\vec{R}_S) = \left| \vec{R}_T - \vec{R}_S \right| + \left| \vec{R}_R - \vec{R}_S \right|$  With constraint:  $g(\vec{S}) = \frac{1}{2} \vec{R}_S^T \mathbf{M} \vec{R}_S = 1,$

## Can also use unit-difference (UD) gradient $\vec{\nabla} J_{UD}(\vec{R}_S) = \hat{q}(\vec{R}_S) - \hat{n}(\vec{R}_S)$ surface normal $\vec{n}$ )

Jales, P. (2012) Ph.D Thesis University of Surrey.

Southwell & Dempster (2018)

0.1109/JSTARS.2017.2775647.

Garrison, et al.(2002) 10.1109/ 36.981349.

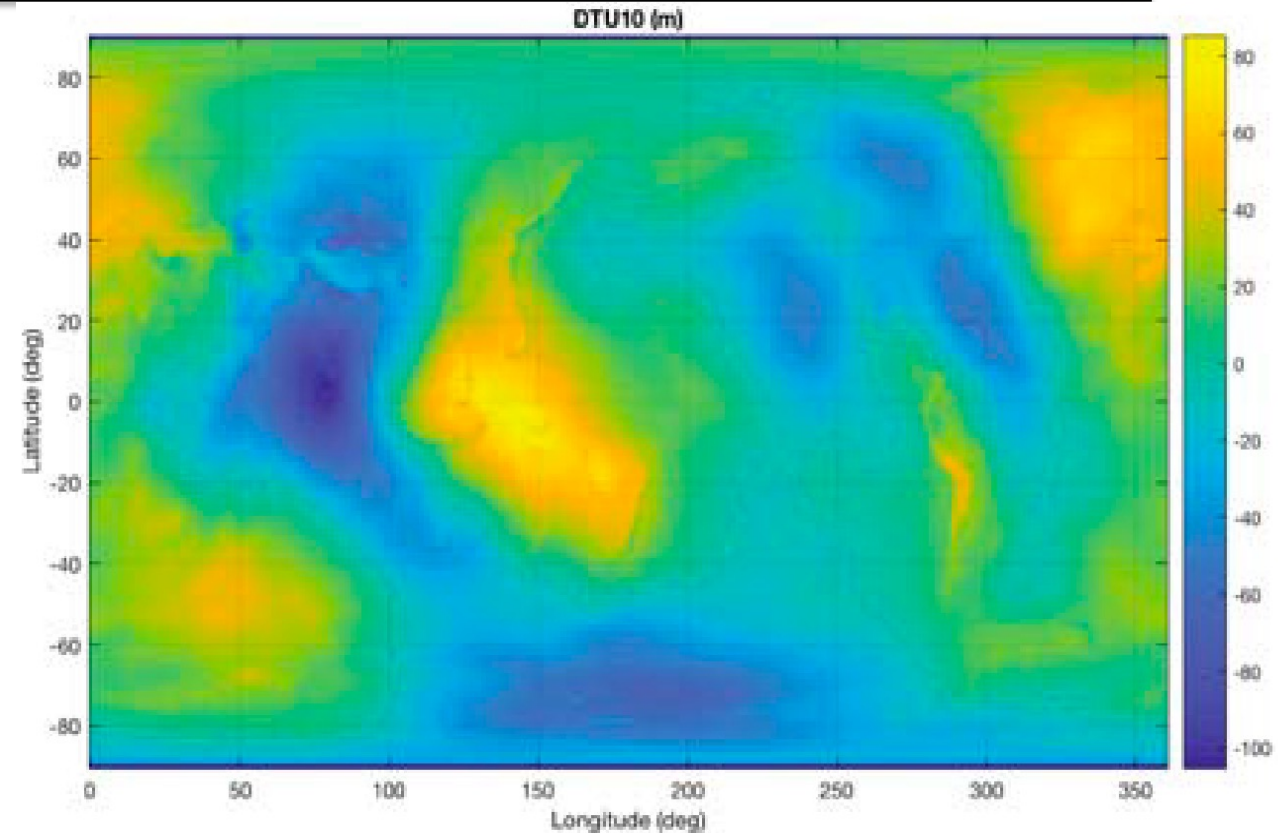
Gordon, W.B. (2014) 10.1109/TAP.2014.2299271



MSL can vary up to +/- 100 m from WGS-84 ellipsoid

100m ht. error @ 30 deg. incidence = 170 m delay error (2.25 CYGNSS DDM pixels)

Grid search using interpolated DTU10\* MSL around Ellipsoidal SP - find min. path delay



DTU10 MSL – WGS84 height adjustment  
[Gleason, et al., S., (2019)  
10.1109/JSTARS.2018.2832981]

\*[National Space Institute (Denmark)]

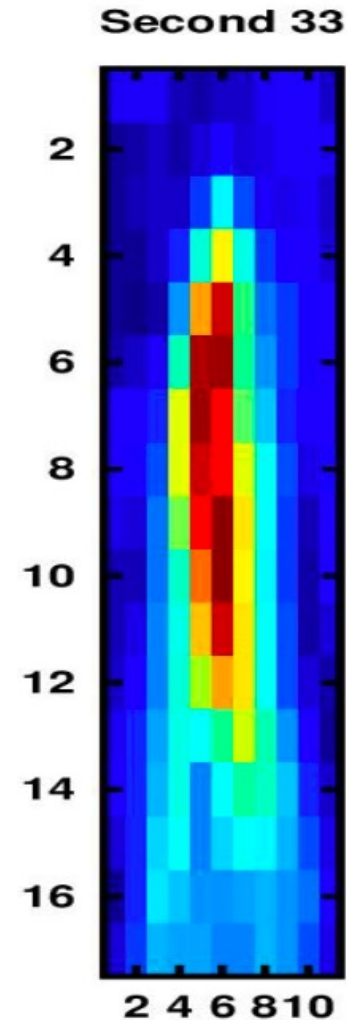
**Terrain is more complex and variable**

Multiple peaks possible

Gleason, et al. (2020)

[10.3390/RS12081317] proposed consistency check:

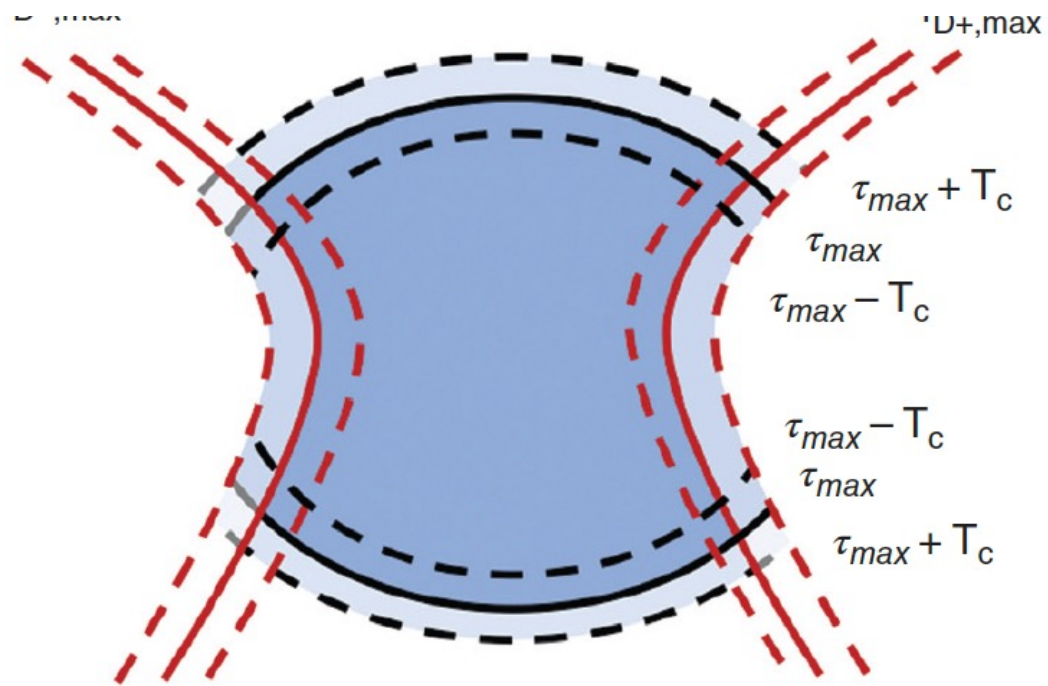
- Delay/Doppler from SRTM DEM
- Snell's law ( $\theta_I = \theta_R$ )



Example of multiple-peak DDM

[Gleason, et al. (2020)  
[10.3390/RS12081317]



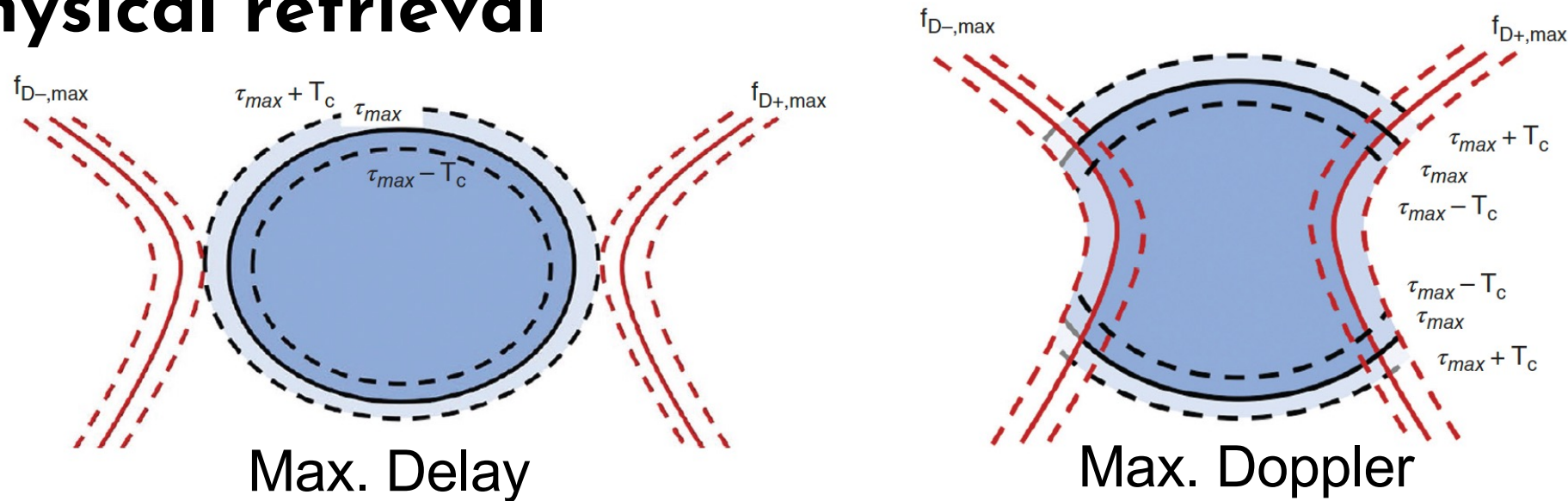


# Spatial resolution and coverage





## Extent of DDM ( $\tau_s: \tau_{\max}, +/- f_{D_{\max}}$ ) used to produce single geophysical retrieval



### Complications:

[PNT in 21<sup>st</sup> Century (10.1002/9781119458449.ch34)]

- Surface not uniformly weighted
- Time averaging will “spread” observation along flight path
- Specular reflection will not “fill” all delay-Doppler samples (“bins”)

# Resolution defined by the DDM

Define as geometric average of semimajor & semiminor axes  
 First delay bin of DDM (assume diffuse scatter)

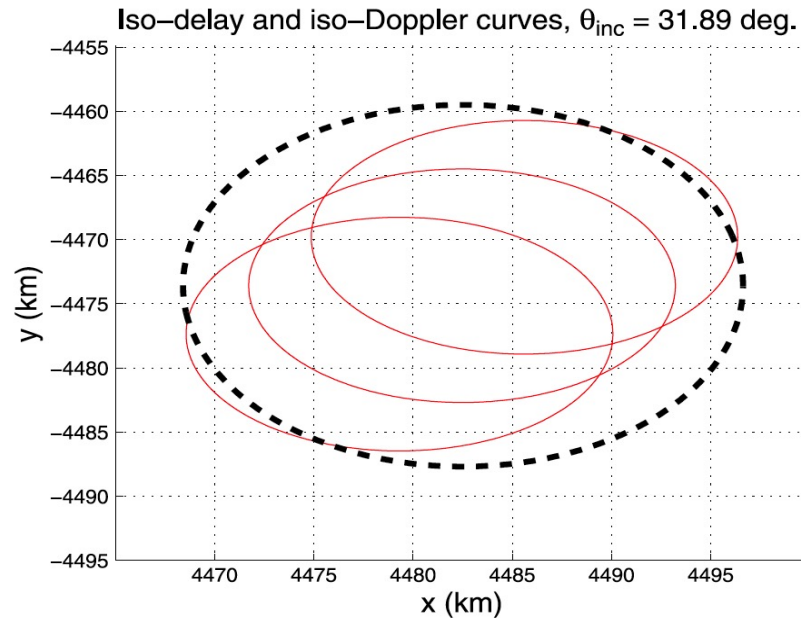
$$R = 2\sqrt{ab}$$

$$\approx 2 \frac{\sqrt{ch(T_c/2)}}{\sin \gamma}$$

Airborne:	B=1.023 MHz (GPS C/A)	B=10.23 MHz (GPS P(Y))	B=400 MHz (DBS)
( $\gamma=30^\circ$ , h=10 km)	4.8 km	1.5 km	219 m
( $\gamma=60^\circ$ , h=10 km)	2.8 km	880 m	126 m
Satellite:			
( $\gamma=30^\circ$ , h=500 km)	34.2 km	10.8 km	1.5 km
( $\gamma=60^\circ$ , h=500 km)	19.8 km	6.3 km	894 m



Often necessary to reduce error  
 “spreads” out resolution area in flight direction.



[Rodriguez-Alvarez & Garrison,  
 10.1109/TGRS.2015.2475317]

- Resolution requirement can set the max. averaging window  
 Surface area can be weighted with BRCS (stronger reflections  
 contribute more to observable) [Clarizia & Ruf, 10.1109/LGRS.2016.2565380]



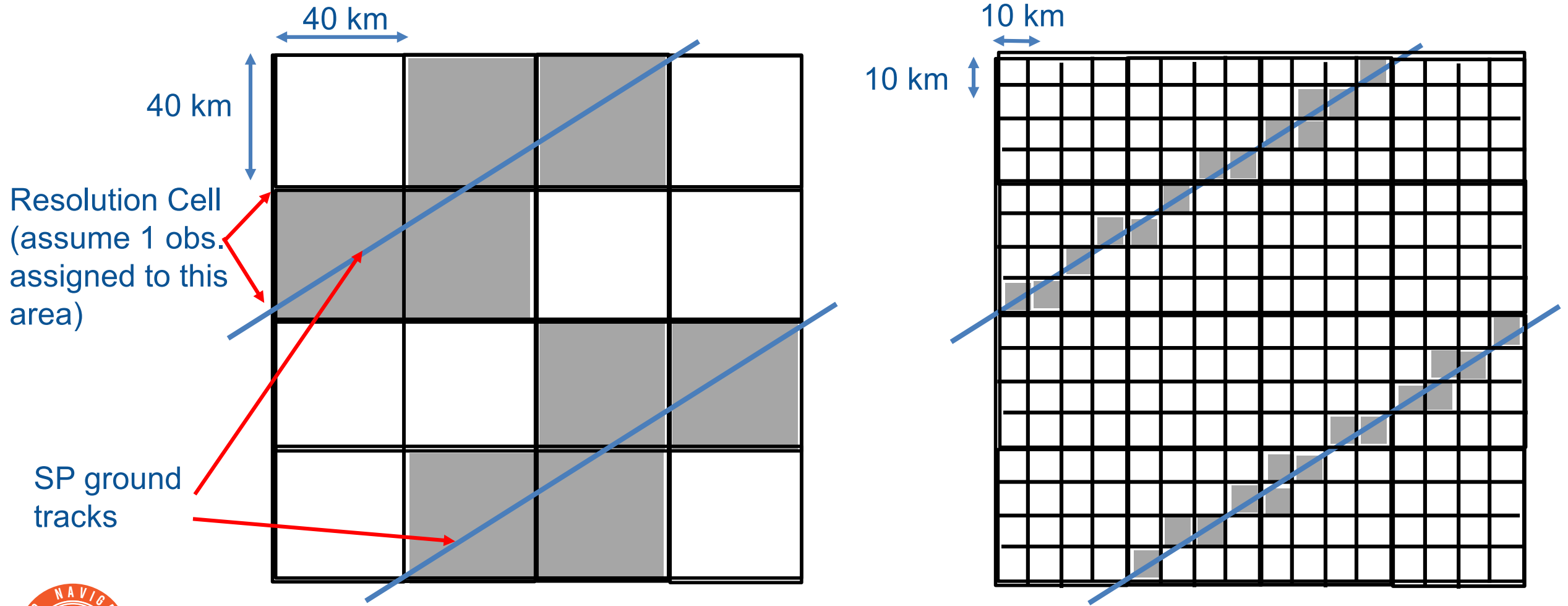
## Resolution approximated by first Fresnel Zone (FFZ)

$$R = 2\sqrt{ab} \approx 2\frac{\sqrt{h\lambda}}{\sin \gamma}$$

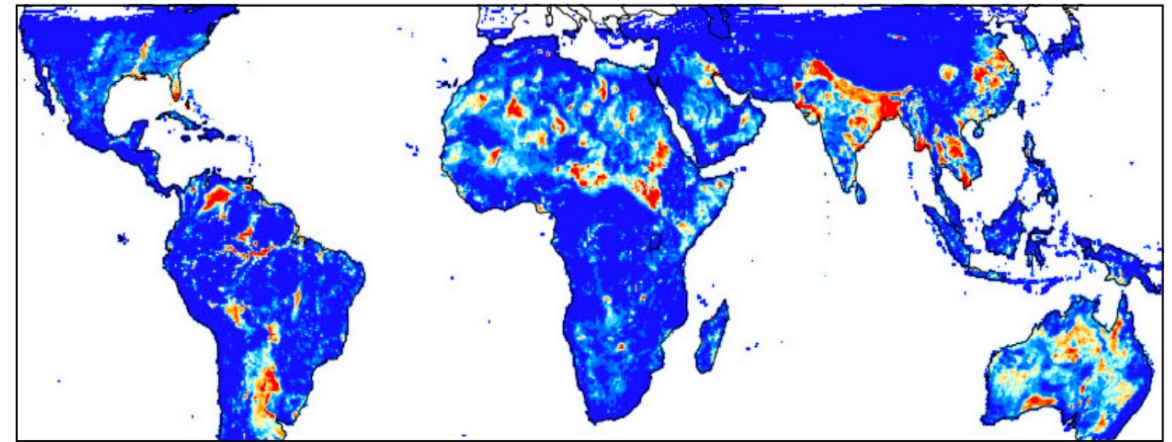
Airborne:	L-band (1.575 GHz)	P-band (360 MHz)	I-band (137 MHz)
( $\gamma=30^\circ$ , h=10 km)	174 m	364 m	592 m
( $\gamma=60^\circ$ , h=10 km)	101 m	210 m	342 m
Satellite:			
( $\gamma=30^\circ$ , h=500 km)	1.2 km	2.5 km	4.2 km
( $\gamma=60^\circ$ , h=500 km)	712 m	1.5 km	2.4 km



## Relationship between resolution and coverage



# Coherence



[Al-Khaldi, et al. 10.1109/TGRS.2020.300978]

**Coherent- Power increase  
proportional to  $T_I$**

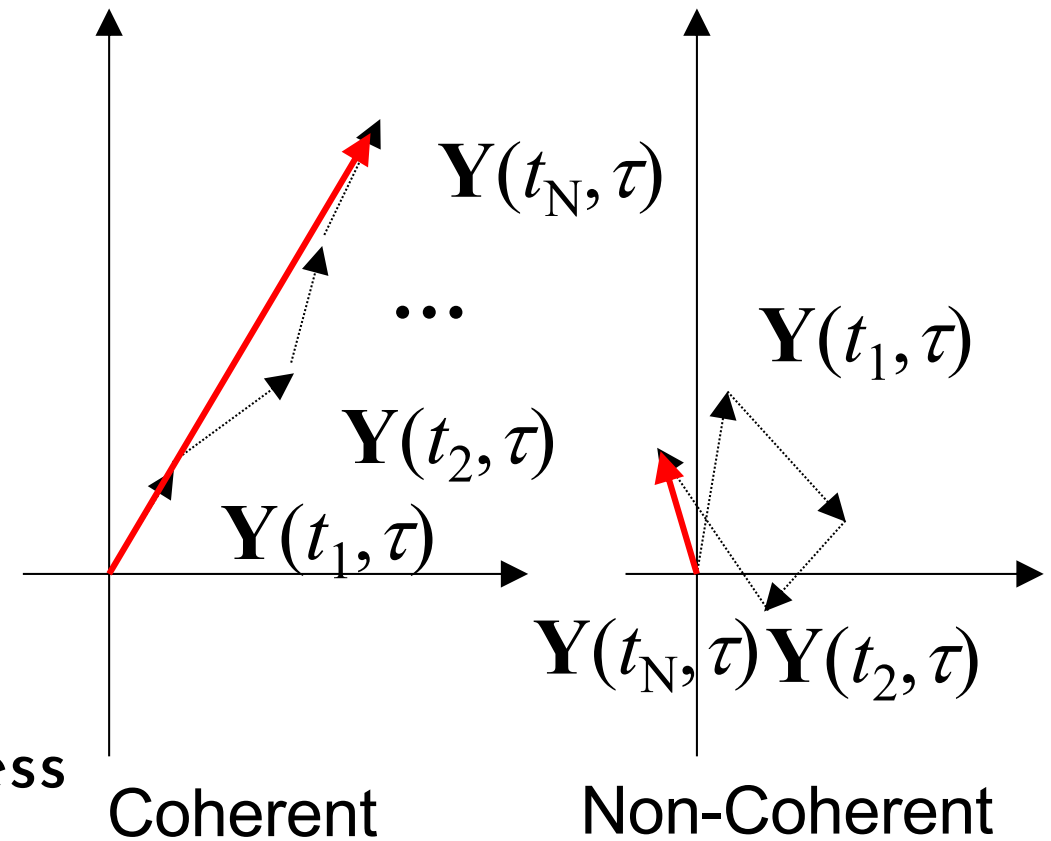
$$\frac{P_{coh,2}}{P_{coh,1}} = \frac{T_{I,2}}{T_{I,1}}$$

**“gold standard” test for coherence**

$$10\log_{10} \left( \frac{P_{T_I}}{P_{1ms}} \right) > \gamma_c$$

- Threshold  $\gamma_c$
- Requires adjustment of  $T_I$  (in practice, access to IF data - not operationally practical)

[Loria, et al., 10.1109/IGARSS.2018.8517441





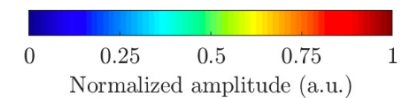
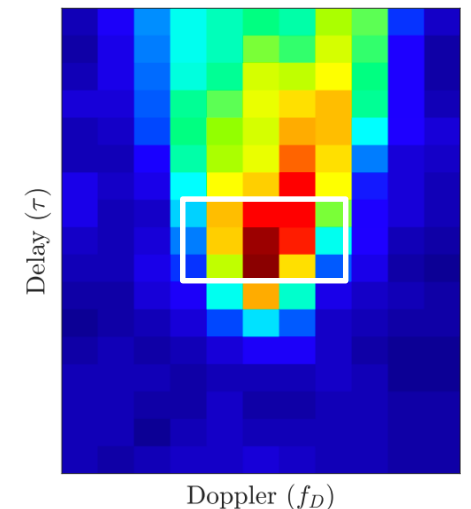
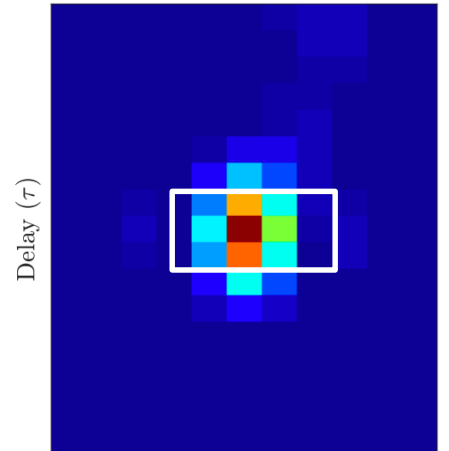
Compares power ratio (PR) to threshold

$$PR = \frac{C_{in}}{C_{out}}$$

Represents power “inside” specular pixels (3X5 for CYGNSS) and “outside” ( $N_t \times N_f$ )

$$C_{in} = \sum_{i=-1}^1 \sum_{j=-2}^2 \text{DDM}(\tau_M + i, f_M + j) \quad C_{out} = \sum_{i=1}^{N_t} \sum_{j=1}^{N_f} \text{DDM}(i, j) - C_{in}$$

- Can be applied to Level 0 “counts”
- Threshold “tuned” through comparison to “gold standard”
- “Outside” region adjusted to avoid noise pixels



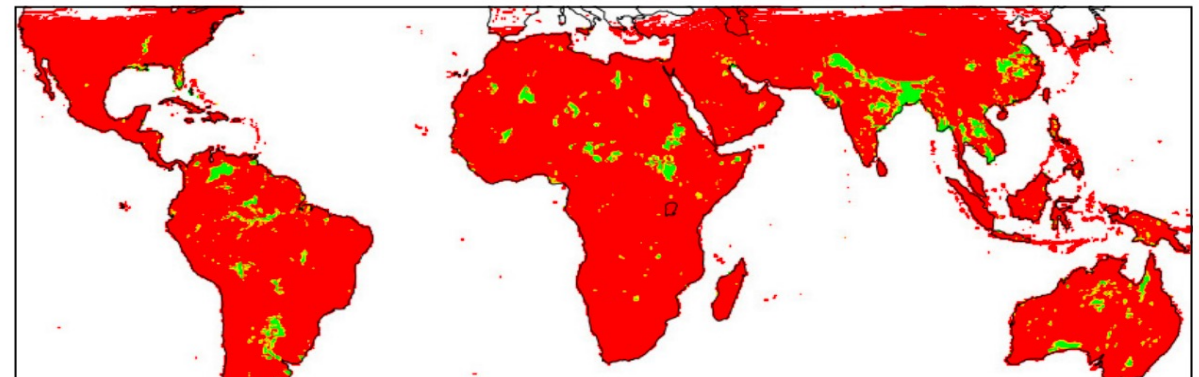
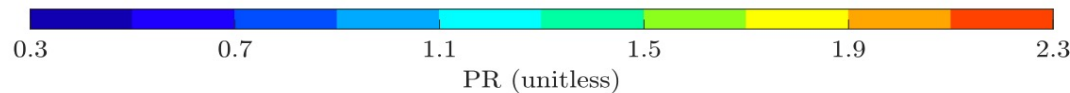
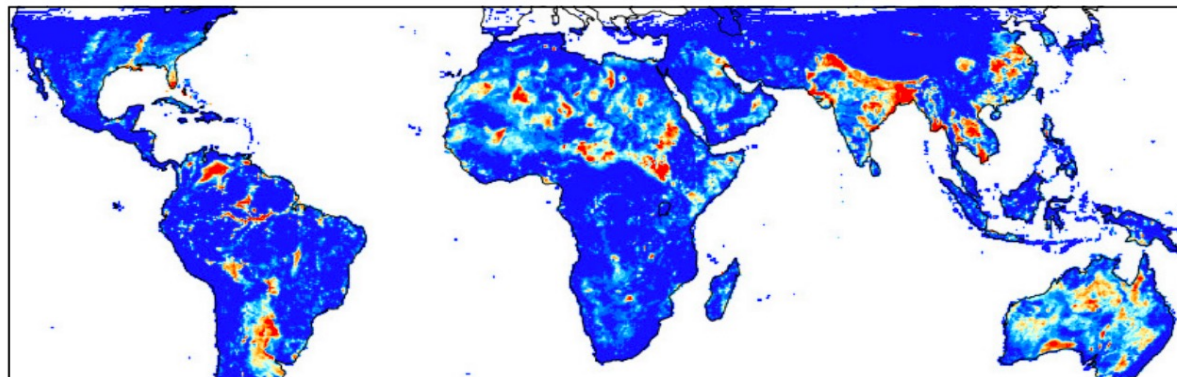
[Al-Khaldi, et al. 10.1109/TGRS.2020.300978]

Tests similarity of DDM to “pure” ambiguity function

$$R = \frac{|\langle Y(\tau, f_D)\chi(\tau, f_D)\rangle|^2}{\langle Y(\tau, f_D)Y(\tau, f_D)\rangle \langle \chi(\tau, f_D)\chi(\tau, f_D)\rangle}$$

Compares correlation (R) to threshold

MFD and DPSD give very similar results



[Al-Khaldi, et al. 10.1109/TGRS.2020.300978]

Coherence modeled using random rough surface

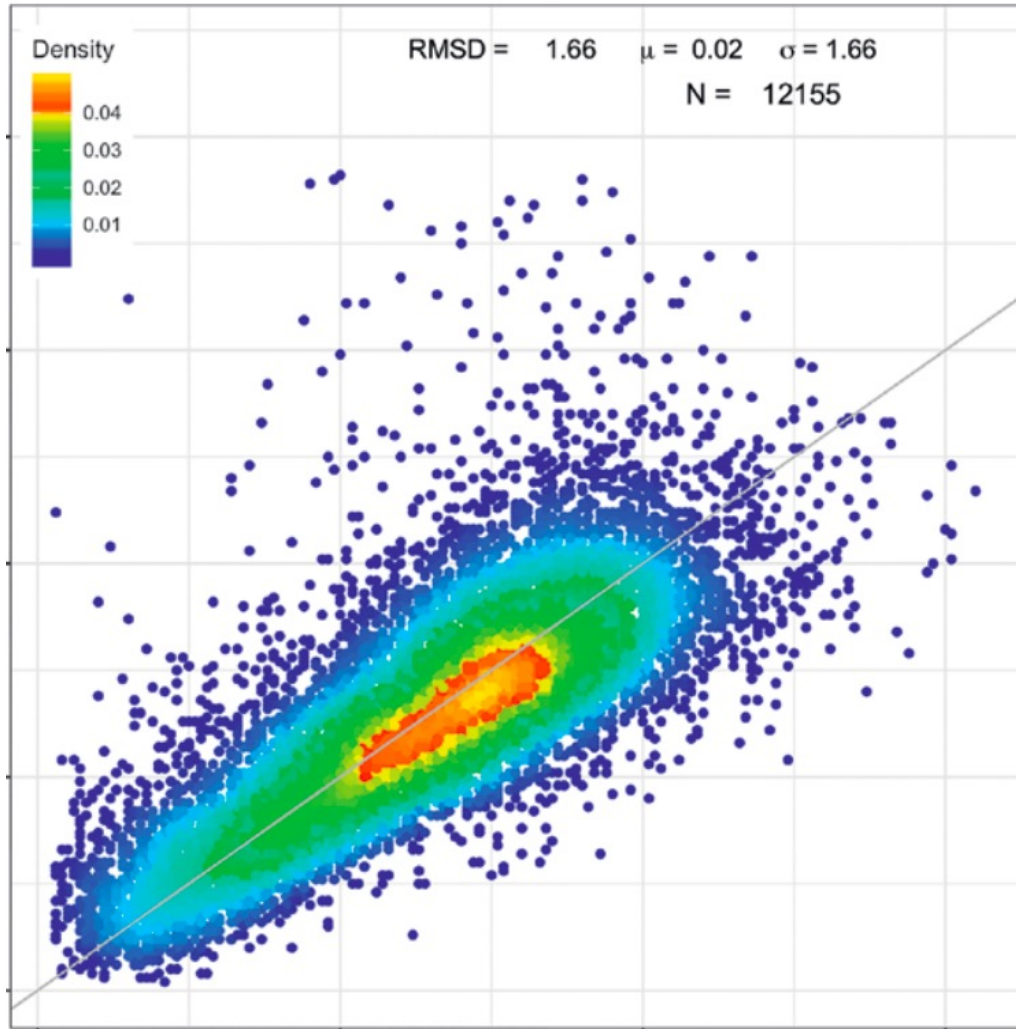
Altitude -size of FFZ in variance computation

Airborne or spaceborne Receiver:

	L-band (1.575 GHz)	P-band (360 MHz)
Ocean Winds ( $U_{10}$ )	2-3 m/s	5-7 m/s
Land surface height RMS	5-7 cm	15-30 cm

Tower (~10-50 m) receiver: Much more coherent

[Balakhder, et al., 10.1109/TGRS.2019.2935257]



# GNSS-R observables



Calibration produces Level 1a DDM's:

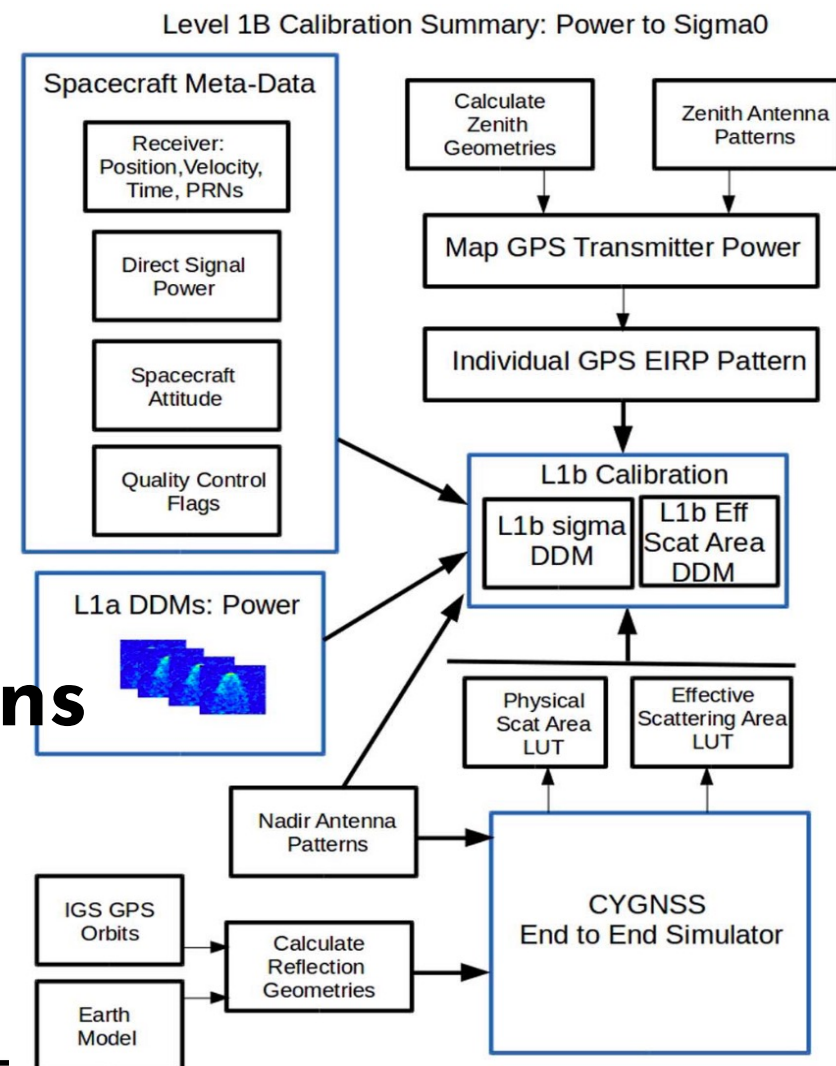
$P(\tau, f)$  [W]

“Unwrap” (Invert) radar equation to give BRCS for each  $(\tau, f)$

$$\bar{\sigma}(\tau, f) = \frac{P(\tau, f)(4\pi)^3 L_{a1} L_{a2} L_{DDMI}(\tau, f) R_R^2 R_T^2}{\lambda^2 P_T G_{T,S} G_{R,S}} \text{ [m}^2\text{]}$$

NBRC observable formed from  $N_\tau \times N_f$  bins

$$\sigma^0 = \frac{\sum_{i=1}^{N_\tau} \sum_{j=1}^{N_t} \bar{\sigma}(\tau_i, f_j)}{\sum_{i=1}^{N_\tau} \sum_{j=1}^{N_t} \bar{A}(\tau_i, f_j)} \text{ [N.D.]} \quad \bar{A}(\tau_i, f_j) = \text{Effective area at } (\tau_i, f_j)$$



## Inversion of Friis' equation

$$\Gamma(\tau, f) = \frac{P_{coh}(\tau, f)(4\pi)^2 L(R_R + R_T)^2}{\lambda^2 P_T, G_{T,S} G_{R,S}}$$

**Coherent reflection only from the specular point.**







**My career began with GNSS!**

(not radiometry, radar or communications)

GNSS orbits: **continuous global coverage**

**L-band:** good penetration of atmosphere, vegetation, rain, etc

... but:

Only penetrates soil ~5cm

Not sensitive to high frequency ( $> \sim 2\pi/(3\lambda)$ ) ocean waves

**Pseudorandom noise (PRN) code** - designed for ranging



## What about other signals ?

---

**Approximately 400 communication satellite Signals of Opportunity (SoOp) in GEO**

**High-powered (~30 dB above GNSS) signals**

**Allocations in most bands used for remote sensing:**

**P,L,S, C, Ku/Ka**

**Designed for data transmission - Not ranging!**

**Assumption: Compression & Encryption are very efficient at filling available spectrum, no periodic components**

- Data is nearly random
- Direct signal can be used as reference (e.g. iGNSS-R)



# Self-Ambiguity Function

Defined by

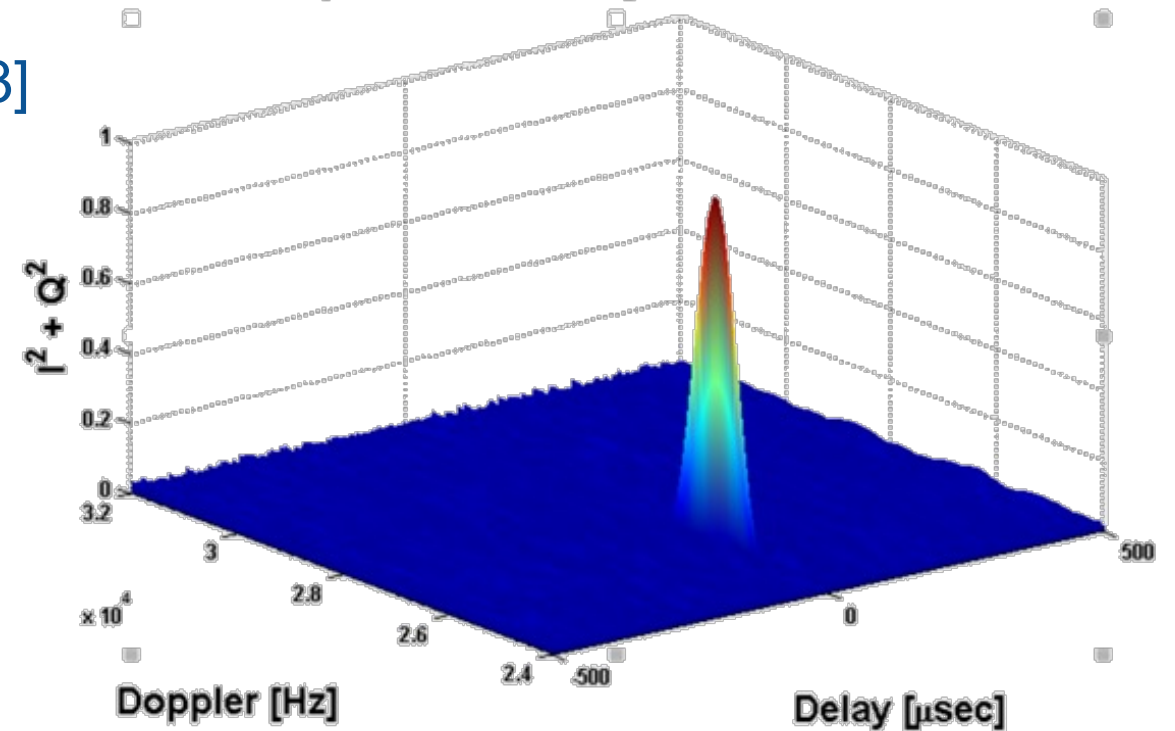
$$|\chi(\tau, f_c)|^2 = \left| \frac{1}{T_I} \int_0^{T_I} s(t) s^*(t - \tau) e^{-j2\pi f_c t} dt \right|^2$$

\*[Baker, et al., 2005, DOI: 10.1049/ip-rsn:20045083]

## Early DBS Experiment



Ambiguity Function for DTV  
 $F_c = 12.224 \text{ GHz}$ ,  $F_s = 50 \text{ MHz}$ , RHCP

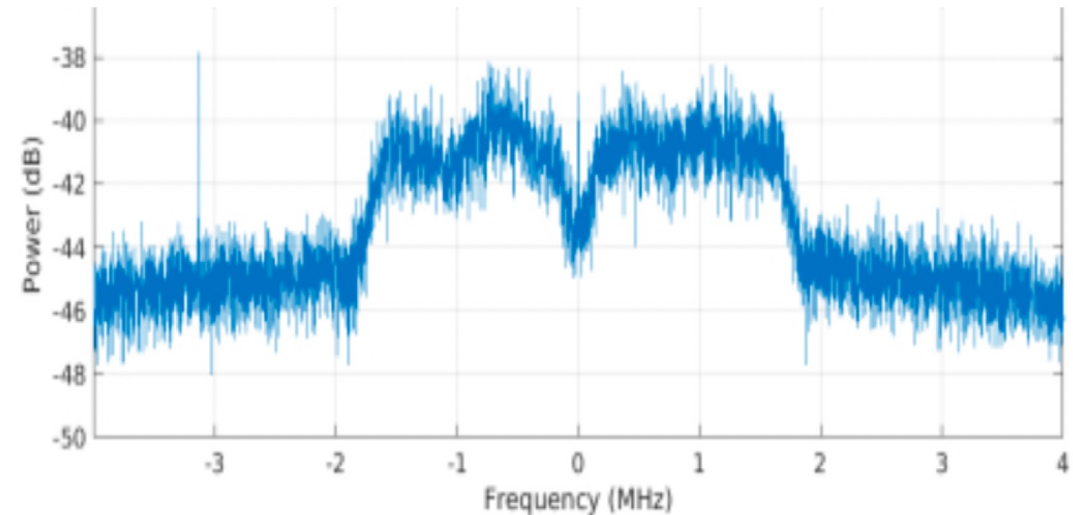


# What else is out there ?

## Link budget comparison ....

	GPS	XM Radio
<b>EIRP (dBW)</b>	<b>24.5</b>	<b>68.5</b>
Frequency (MHz)	1575.4	2342.2
Atmos. Loss (dB)	-2.0	-3.0
Range (km)	20200.0	35888.0
Space Loss (dB)	-157.1	-162.1
Power Density (dB/m <sup>2</sup> )	-134.6	-96.6
EAI A	-25.4	-28.8
Antenna Gain (dBm <sup>2</sup> )	3.0	3.0
Received Power (dBW)	-157.0	-122.4
Noise Temp (K)	290.0	290.0
Bandwidth (MHz)	2.0	2.0
<b>SNR (dB)</b>	<b>-16.0</b>	<b>18.5</b>

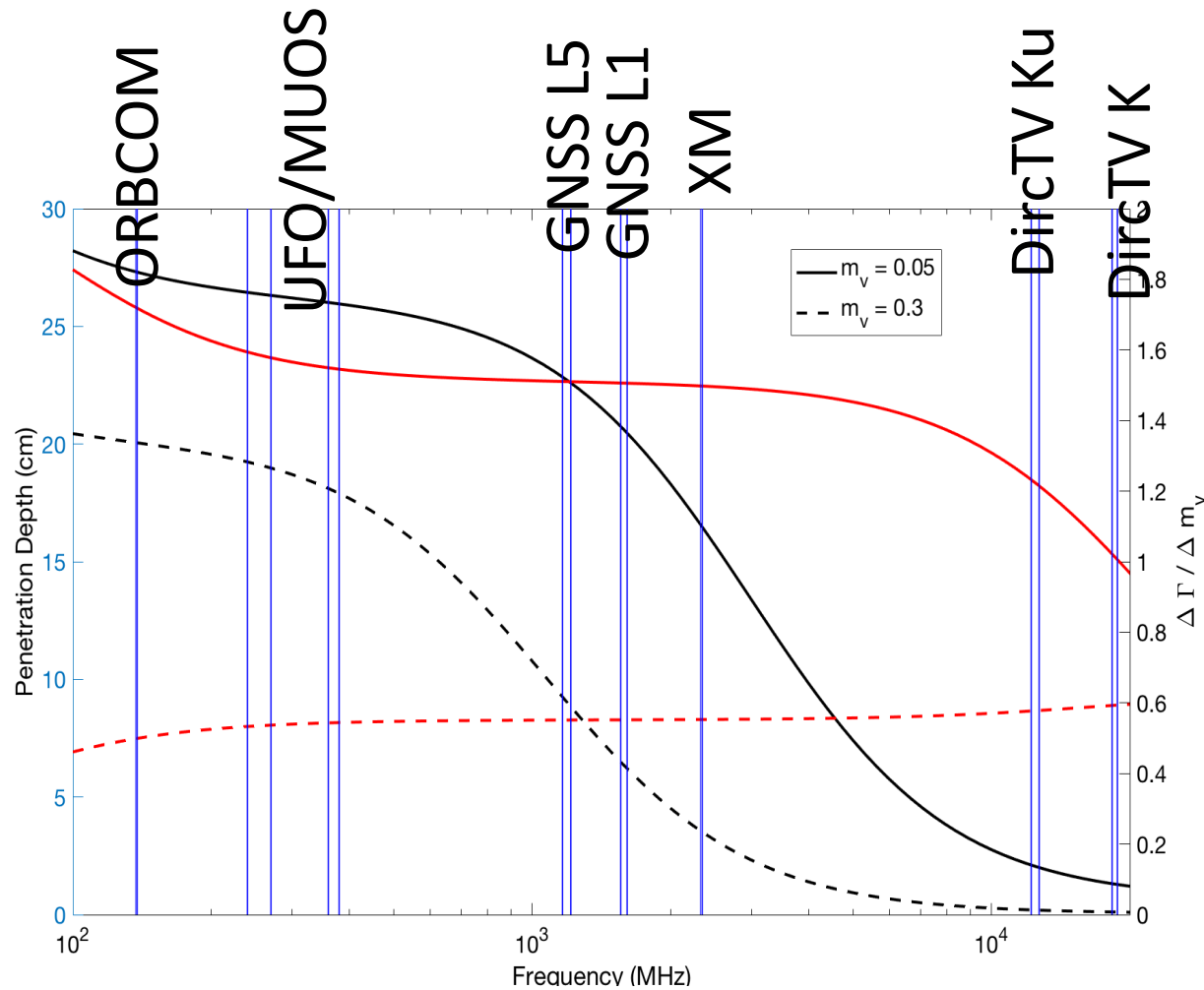
XM-Radio spectrum (@ receiver)



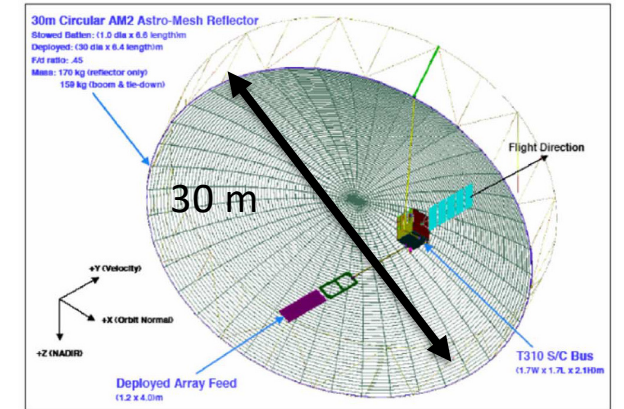
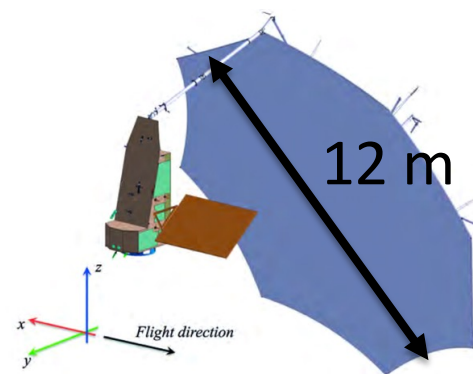
Very high SNR possible with communication signals!



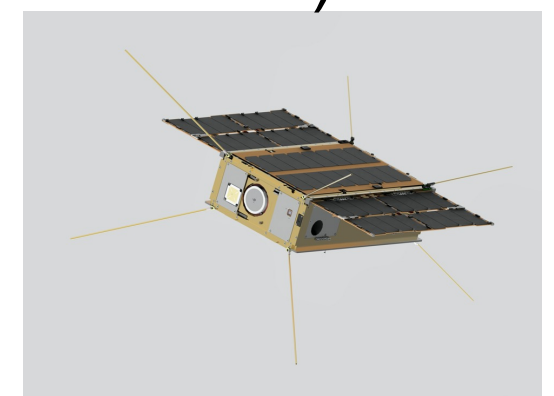
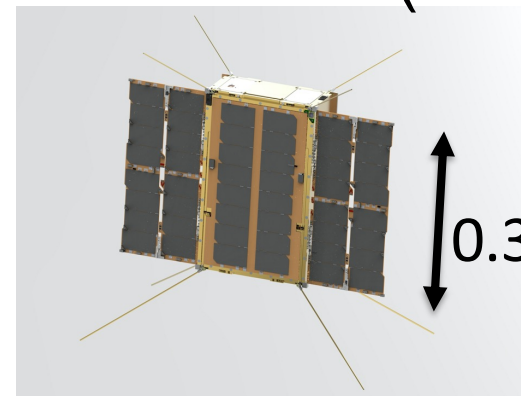
# Frequencies < 500 MHz (P-band)



BIOMASS (435 MHz) MOSS (137 MHz)

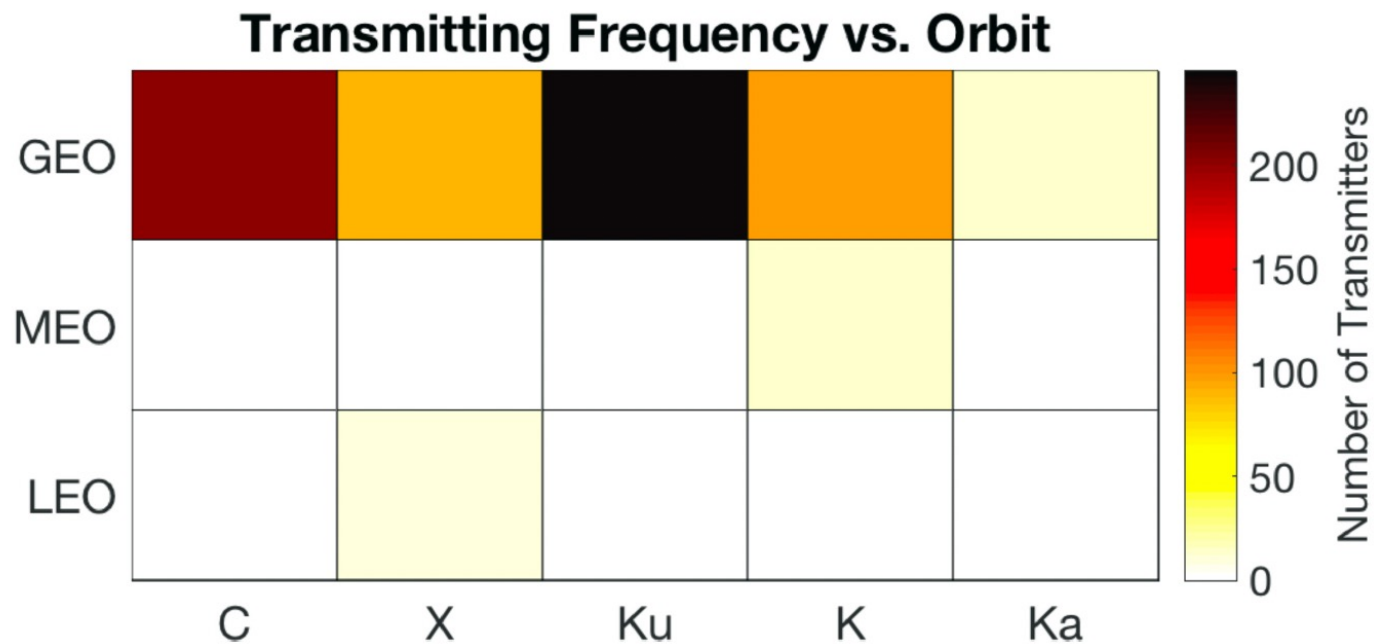


SNOOPI (255 & 370 MHz)





## Wide bandwidth, Good coastal coverage



System	Frequency (GHz)	BW (MHz)
DirecTV	12.5 (Ku)	500
	18.6 (K)	500
Astra-4a	12.2 (Ku)	1050
	20.3 (Ka)	200
AEHF	20.7 (Ka)	1000

[Benveniste et al., 10.3389/fmars.2019.00348]



## Altimetry error dependence on bandwidth

